

Design and Implementation of a Mobile Robot

by

Yeap Kim Ho

Dissertation submitted in partial fulfillment of
the requirements for the
Bachelor of Engineering (Hons)
(Electrical and Electronics Engineering)

JUNE 2004

Universiti Teknologi PETRONAS
Bandar Seri Iskandar
31750 Tronoh
Perak Darul Ridzuan

CERTIFICATION OF APPROVAL

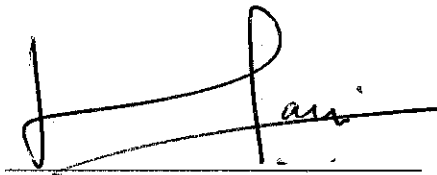
DESIGN AN IMPLEMENTATION OF A MOBILE ROBOT

by

Yeap Kim Ho

A project dissertation submitted to the
Electrical & Electronics Engineering Programme
Universiti Teknologi PETRONAS
in partial fulfilment of the requirement for the
Bachelor of Engineering (Hons)
(Electrical & Electronics Engineering)

Approved:

A handwritten signature in black ink, appearing to read 'Mohd Haris Md Khir', is written over a horizontal line.

(MOHD HARIS MD KHIR)

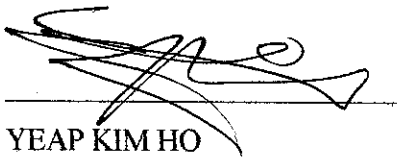
Project Supervisor

UNIVERSITI TEKNOLOGI PETRONAS
TRONOH, PERAK

June 2004

CERTIFICATION OF ORIGINALITY

This is to certify that I am responsible for the work submitted in this project, that the original work is my own except as specified in the references and acknowledgements, and that the original work contained herein have not been undertaken or done by unspecified sources or persons.



YEAP KIM HO

ACKNOWLEDGEMENTS

This project would be insurmountable had it not been for the help, support and advices given by a number of people. Thus, the writer would like to take this opportunity to express his profound gratitude to each and every one of them.

Firstly, the writer is profusely grateful to his family, especially both his parents – Yeap Tang Kee @ Yeap Peng Keat and Pon Moy for giving him love and supports all the while. He is indeed fortunate for being able to born in a family teeming with care and solicitude. The writer felt sorry for not able to spare much time to be with them as he has put much attention on his final year project. He hoped that he would be able to make up for them in the years to come. The writer is also thankful to his siblings – his 2 sisters, Yeap Chee Beng and Yeap Juan Juan and his twin brother, Yeap Kim Huat. Their support has been a great source of motivation to him.

Secondly, the writer would like to convey his heartfelt thankfulness to his supervisor – Mr. Mohd Haris Md Khir. Throughout the entire project, Mr. Haris has been guiding him all along and giving him invaluable advices to cope with every predicament that the writer faced. For that, the writer felt greatly indebted to him. The writer is grateful to have worked under Mr. Haris's supervision. He has learned a lot throughout the process of accomplishing his project.

Lastly but definitely not the least, the writer is sincerely thankful to everyone that has been helping him out to make this project a successful one. He realizes that the project does not belong to him alone as it may not be completed without the help and support from his friends, supervisor, and his loved ones.

ABSTRACT

A robot is a mechanical device, which possesses the capability of emulating a human's characteristic in some way or another. The project is to build a mobile robot, which should be able to avoid any encumbrances, while at the same time, is capable of maneuvering at a predetermined path. The mobile robot should be intelligent enough to make decisions as to which direction it is to turn when it reaches a certain situation – ie. a turning point, a T-junction, a dead end, etc. An extensive research would be conducted first before starting off designing the robot. Subsequently, the exact materials would be selected. The structure of the mobile robot would then be designed and built. The main circuitries required to construct a mobile robot include ultrasonic sensors, a pair of H-bridge circuits, and a microcontroller circuit. The ultrasonic sensors serve as eyes for the robot. They help to detect obstacles en route. The purpose of constructing the H-bridge circuit is to control the rotational direction of the motors. The microcontroller plays a most essential role in the mobile robot. The microcontroller acts as a brain for the mobile robot and would be making decisions on how the robot should react when it encounter obstacles. Due to its simplicity and the ease in getting familiarized with, an 8-bit PIC16F84A microcontroller is implemented for the project. The components – that is, the sensors, motors, the H-bridge circuits, and the microcontroller, would be validated individually first, before integrating them onto the mobile robot. The program of the microcontroller would be written in assembly code form and would then be validated. Lastly, successive validation tests would be conducted on the entire robot to ensure the reliability of the mobile robot.

TABLE OF CONTENTS

CERTIFICATION OF ORIGINALITY	i
ACKNOWLEDGEMENT	ii
ABSTRACT	iii
TABLE OF CONTENTS	iv
LIST OF FIGURES	vi
LIST OF TABLES	vii
LIST OF APPENDICES	viii
1. CHAPTER 1: INTRODUCTION	1
1.1 Background of Study	1
1.2 Problem Statement	1
1.2.1 Problem Identification	1
1.2.2 Significance of the Project	1
1.3 Objectives and Scope of Studies	2
1.3.1 Objectives	2
1.3.2 Scope of Studies	2
2. CHAPTER 2: LITERATURE REVIEW	4
2.1 Structure References	4
3. CHAPTER 3: THEORY	7
3.1 Direction Control of the Mobile Robot	7
3.1.1 Operation Mode of the Mobile Robot	7
3.2 H-bridge Circuit	8
3.2.1 MOSFET Overview	9
3.2.2 Operational Mode of an H-bridge Circuit	10
3.3 Ultrasonic Sensors	13
3.4 PIC16F84A Microcontroller	15

4.	CHAPTER 4: METHODOLOGY/ PROJECT WORK	17
4.1	Procedure Identification	17
4.1.1	Stage 1: Building Robot's Structure	18
4.1.2	Stage 2: Constructing H-bridge Circuit	19
4.1.3	Stage 3: Programming PIC16F84A microcontroller	19
4.1.4	Stage 4: Constructing Ultrasonic Sensors	20
4.1.5	Stage 5: Programming Path Finding Algorithm	20
4.1.6	Stage 6: Integrating and Validating	21
4.2	Tools/ Components	21
5.	CHAPTER 5: RESULT AND DISCUSSION	22
5.1	Structure Design	22
5.1.1	Front View	22
5.1.2	Side View	23
5.1.3	Bottom View	23
5.1.4	Snap Photos of Overall Design	24
5.2	H-bridge Circuit in Printed Circuit Board	25
5.2.1	PSPICE Schematic	25
5.2.2	PCB Layout	26
5.3	H-bridge Calculation	27
5.3.1	Maximum Torque	27
5.3.2	Normal Torque	31
5.3.3	The Effect of Loads on I_D , V_{GS} , and V_{DS}	32
5.3.4	Discussion	35
	An Analysis on Maximum and Normal Torque Performance	35
	An Analysis on the Effect of Loads on a H-bridge Circuit	36
5.4	Ultrasonic Sensors	38
5.4.1	Transmitter	38
5.4.2	Receiver	40
5.4.3	Discussion	44
5.5	Features of the Mobile Robot	45

5.5.1	Obstacles Avoidance	45
5.5.2	Path Finding	47
5.5.3	Discussion	51
	Problems Encountered and Method of Corrections	51
6.	CHAPTER 6: CONCLUSION	52
	REFERENCES	xi
	APPENDICES	xii

LIST OF FIGURES

- Figure 3.1 H-bridge circuit
- Figure 3.2 Transfer characteristic curves for N-channel and P-channel MOSFETs
- Figure 3.3 Standard symbols for an N-channel and a P-channel Power MOSFET
- Figure 3.4 Stop mode
- Figure 3.5 Clockwise direction
- Figure 3.6 Counterclockwise direction
- Figure 3.7 Shoot through current
- Figure 3.8 Ultrasonic transmitter
- Figure 3.9 Ultrasonic receiver
- Figure 3.10 The pin diagram of a PIC16F84A microcontroller
- Figure 5.1 Front view of the mobile robot
- Figure 5.2 Side view of the mobile robot
- Figure 5.3 Bottom view of the mobile robot
- Figure 5.4 Overall picture of the mobile robot
- Figure 5.5 Front and back view of the mobile robot
- Figure 5.6 Side view of the mobile robot
- Figure 5.7 H-bridge schematic
- Figure 5.8 PCB layout
- Figure 5.9 On-region characteristic for MTP2955V Power MOSFET
- Figure 5.10 On-region characteristic for MTP3055V Power MOSFET
- Figure 5.11 ID vs Load
- Figure 5.12 P-channel V_{GS} vs Load
- Figure 5.13 P-channel V_{GS} vs Load
- Figure 5.14 N-channel V_{GS} vs Load
- Figure 5.15 N-channel V_{DS} vs Load
- Figure 5.16 A 555 timer diagram
- Figure 5.17 Waveform from a 400st ultrasonic transmitter

- Figure 5.18 Non-inverting amplifier
- Figure 5.19 A plot of the measured values of $V_{out(p)}$ versus distance
- Figure 5.20 Op-amp used as a comparator
- Figure 5.21 Predetermined path for a mobile robot
- Figure 5.22 Pulses supplied to the H-bridge circuit in stage 1
- Figure 5.23 Pulses supplied to the H-bridge circuit in stage 2
- Figure 5.24 Pulses supplied to the H-bridge circuit in stage 3
- Figure 5.25 Pulses supplied to the H-bridge circuit in stage 4

LIST OF TABLES

Table 5.1	Values measured for I_D and V_{DS}
Table 5.2	Results for I_D , V_{GS} , and V_{DS} in different loads
Table 5.3	$V_{in(p)}$ versus $V_{out(p)}$ calculated and $V_{out(p)}$ measured
Table 5.4	Reference voltage
Table 5.5	Decisions taken by the mobile robot at different situations

LIST OF APPENDICES

- APPENDIX A ALGORITHM FOR OBSTACLES AVOIDANCE
- APPENDIX B SOURCE CODE FOR OBSTACLES AVOIDANCE AND PATH FINDING
- APPENDIX C MTP2955V P-CHANNEL MOSFET DATASHEET
- APPENDIX D MTP3055V N-CHANNEL MOSFET DATASHEET

CHAPTER 1

INTRODUCTION

1.1 Background of Study

A robot is a software-controllable man made device that uses sensors to guide itself and/or its end-effector through deterministic motions in order to manipulate physical objects (Shilling 1990). In simple English, it basically means that a robot is a mechanical device built to perform human tasks or to act in a human-like manner. It is built with the intention of mitigating a human's burden or to extend out of a human's capability in order to accomplish tasks, which may seem insurmountable for a human to undertake.

1.2 Problem Statement

1.2.1 Problem Identification

The robot to be built is a mobile robot that is capable of maneuvering by itself on a predefined route. The mobile robot should consist of the following features:

- (i) Avoiding collision with obstacles
- (ii) Making decision on the direction at which it is to turn
- (iii) Traveling from 1 predetermined point to another without encumbering any blockages.

1.2.2 Significance of the Project

This project serves as a fundamental structure whereby future enhancements would be performed on the mobile robot from time to time in order to improve the features

in the robot. Features such as trajectory programming systems and vision systems are proposed as some of the follow-up projects to improve the functionalities of the robot.

1.3 Objectives and Scopes of Studies

1.3.1 Objectives

- (i) To design a robot which is able to navigate at free will while at the same time is able to avoid any impediments on its way.
- (ii) To design a robot which is able to distinguish the route it is traveling and maneuver from 1 predetermined destination to another.
- (iii) To develop a firm and functional mobile robot for future features enhancement purposes.

1.3.2 Scope of Studies

In order to ensure that the mobile robot to be built would be operational, an extensive study has to be conducted on the following areas:

- (i) The structure of existing mobile robot. References are required to be made on existing mobile robots projects in order to learn the way a firm and steady structure is constructed.
- (ii) References are made on the theories of how existing robots operate. References are necessary as it helps to ensure that the operation theory adopted would be applicable.
- (iii) H-bridge circuit is to be built in order to control the direction of the motors. The working theories of the circuit is required to be studies upon before constructing it.

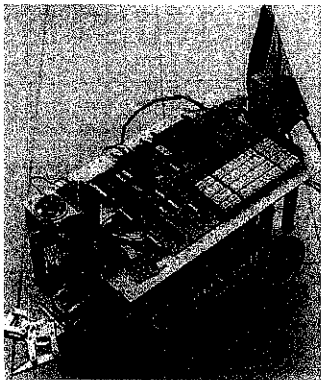
- (iv) Sensors would be implemented for obstacles detection. Thus, it would be important to learn how does a normal ultrasonic circuit functions.
- (v) The PIC16F8X microcontroller has to be studied upon. The microcontroller serves as a medium for the sensors to communicate with the motors – such that, the mobile is able to determine which direction it is to turn when it detects obstacles.
- (vi) Path finding algorithm has to be studied upon. The path finding algorithm would be written in assembly language and flashed into the PIC16F8X chip in order to allow the robot to travel from 1 predefined point to another.

CHAPTER 2

LITERATURE REVIEW

2.1 Structure References

The first step in building a mobile robot is to construct a solid and firm structure. As such, several available models have been referred to before starting off designing the structure of the mobile robot. The following is an overview of some available robots.



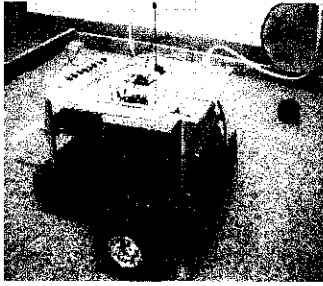
(i) Robot Name: Silverbot¹

Silverbot is a final year Mechatronic Engineering project at Monash University. The mobile robot can wander around without hitting any obstacles or navigating according to a preprogrammed route. It can also respond to a key pressed in the host computer such as moves forward, measures distance, tilts the wireless camera, or grips an object.

(ii) Specifications

- Intel 8051 microcontroller
- Infrared sensor
- Limit switches
- Mechanical gripper (2-axis)
- Radio modem
- Servo motors
- Stepper motors
- Speaker system for alarm output
- Ultrasonic sensor
- Wireless video color camera
- 12 V Lead acid batteries

Source is taken from <http://yoyo.monash.edu.my/~kokleong>



(i) Robot name: Max²

Max, the robot is designed by the Network-centric Applied Research Team (N-CART) from the Ryerson Polytechnic University, Canada. Max can be controlled via a Java-enabled netscape web browser communicating through IP network. The robot streams video images via analog radio link from an on board camera to a web server.

(ii) Specifications

- MC68HC11 micro-controller
- B/W CCD camera



(i) Robot name: Sandwich³

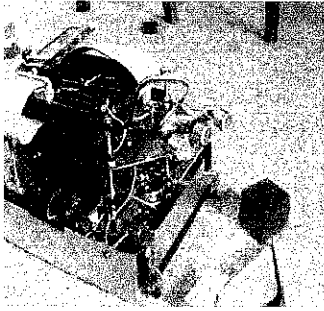
Sandwich is capable of following lines that has a contrast color (either darker or lighter) than the background flooring color.

(ii) Specifications

- infrared sensors
- cadmium sulfide photoresistors
- LEDs
- 6 V rechargeable alkaline batteries
- LEGO wheels

Source is taken from http://dec1.wi-inf.uni-essen.de/~astephan/FIRC2000/s_8.html

Source is taken from <http://www.robotroom.com/Sandwich.html>

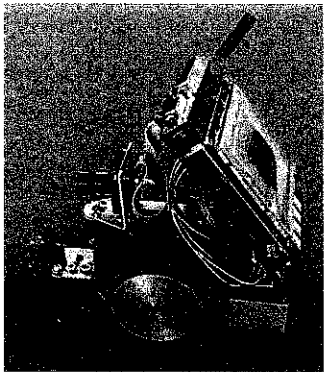


(i) Robot name: Snuf⁴

Snuf was built by Jaap Havinga. It is capable of gathering small building blocks and bringing them to a predefined location. It can avoid any encumbrances while moving around.

(ii) Specifications

- 2 stepper motors
- 12 V Nickel Cadmium batteries
- i386 board
- front bumper
- rotating stereo ultrasound transmitter/receiver



(i) Robot name: Soccerbot⁵

Soccerbot was designed and built by Joker Robotics – a company established in Germany and has its headquarter in Australia. Soccerbot is built specifically for Robocup F180 league. It is completely autonomous.

(ii) Specifications

- EyeBot Controller
- Full mechanics with camera pan and kicker mechanisme
- 2 dc motors with encapsulated gears and encoders
- 2 servos with metal gears for camera and kicker operation
- 3 infra-red PSDs EyeCam digital camera
- Li Ion battery with main charger (85 – 230V)

Source is taken from <http://www.havingasoftware.nl/robot/snuf/snuf.html>

source is taken from <http://www.joker-robotics.com/eyebot/socbot.html>

CHAPTER 3

THEORY

3.1 Direction Control of the Mobile Robot

The mobile robot is designed such that it is able to navigate freely without colliding with any obstacles. Upon detecting an object the mobile robot is capable of changing its direction in order to avoid running into the object.

In short, the mobile robot is supposed to be able to maneuver forward, backward, and turning left and right. Thus, a circuit is required in order to control the rotation direction (either clockwise or counterclockwise) of the motors. In this case, an H-bridge circuit is implemented to control the direction of the motor.

3.1.1 Operation Mode of the Mobile Robot

Forward Mode

Both the motors would be turning in the opposite direction – that is, the motor at the left would be turning counterclockwise; whereas the motor at the right would be turning clockwise.

Reverse Mode

Both the motors would be turning in the opposite direction – the left motor would be turning clockwise; while the right motor would be turning counterclockwise.

Turning Left Mode

Both the 2 motors would be turning in the clockwise direction.

Turning Right Mode

Both the 2 motors would be turning in the counterclockwise direction.

3.2 H-Bridge Circuit

An H-bridge configuration is implemented in order to allow control over rotation torque and direction of the motors in the mobile robot. The circuitry of the H-bridge circuit is shown in Figure 3.1.

As can be seen, the H-bridge circuit consists of 4 main components – N-channel MOSFETs, P-channel MOSFETs, NPN BJT transistors, and PNP BJT transistors. Both the transistors and the Power MOSFETs work as switches that control the flow of current.

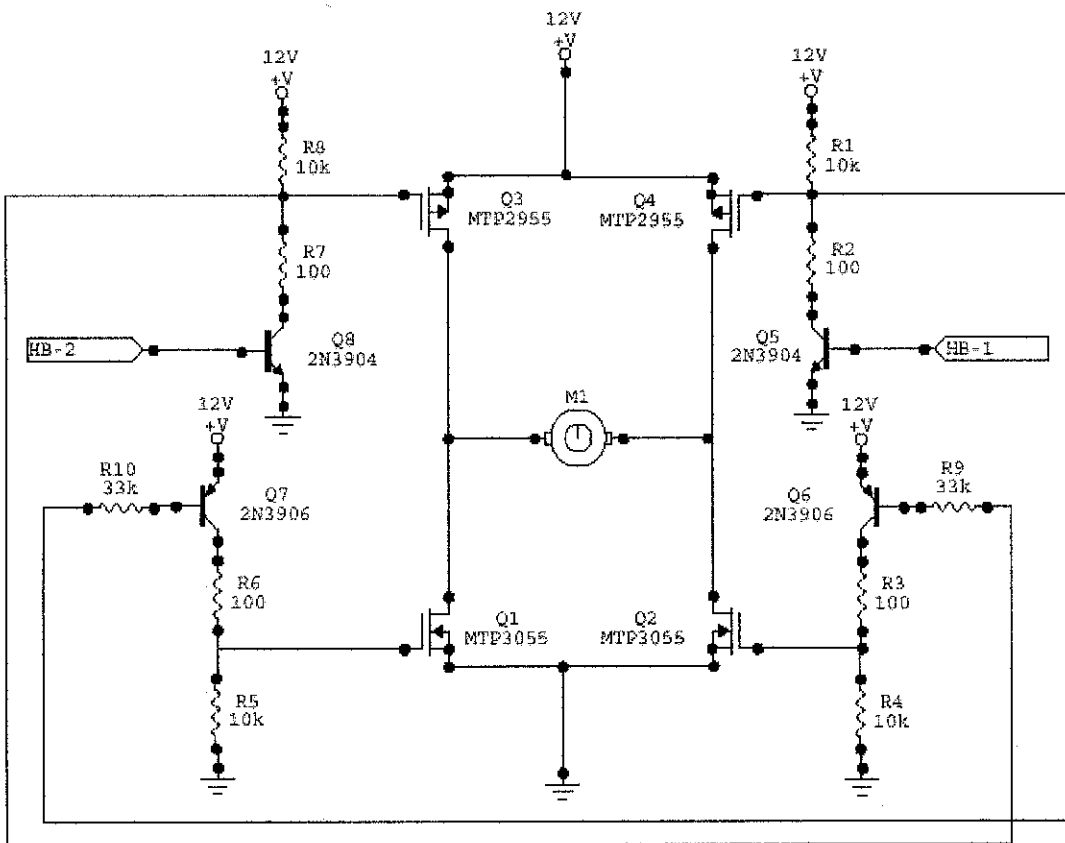


Figure 3.1 H-bridge circuit

3.2.1 MOSFET Overview

4 MOSFETs are implemented in the circuit as switches. A MOSFET would be switched on by applying a voltage to the Gate. The input Gate-to-source voltage controls the output Drain current – a characteristic known as the forward transfer conductance (transconductance). For an N-channel MOSFET, when a positive voltage greater than the Gate-to-source threshold voltage is applied, the N-channel MOSFET would be turned on. Similarly, for a P-channel MOSFET, when a negative voltage greater than the negative Gate-to-source threshold voltage is applied, the P-channel MOSFET would be turned on. The transfer characteristic curve for an N-channel and a P-channel MOSFET is shown in Figure 3.2 below.

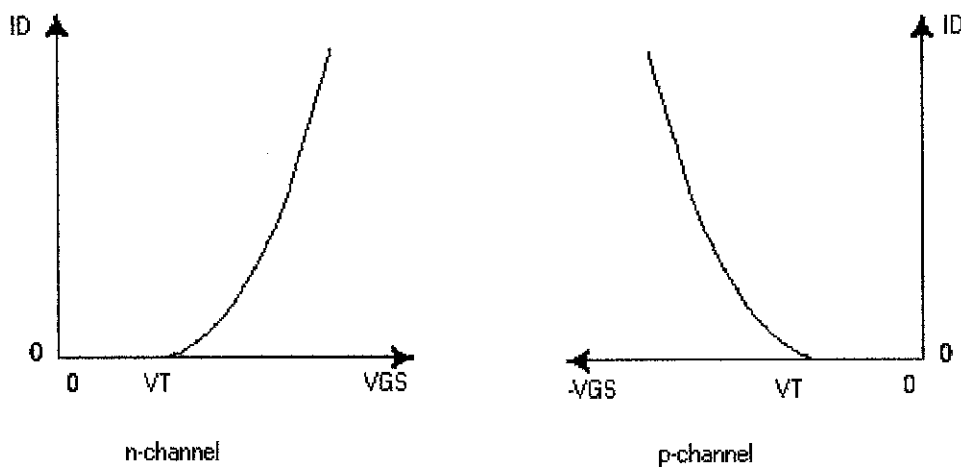


Figure 3.2 Transfer characteristic curves for N-channel and P-channel MOSFETs

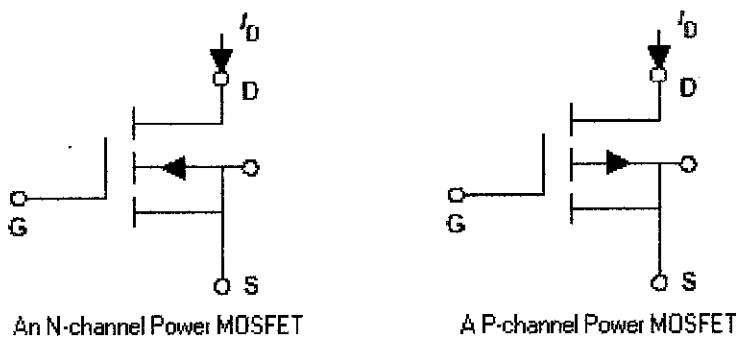


Figure 3.3 Standard symbols for an N-channel and a P-channel Power MOSFET

3.2.2 Operational Mode of an H-bridge Circuit

Stop Mode

When HB-1 and HB-2 is at 0V (grounded), both the 2 BJT transistors – Q8 and Q5 act as an open switch. A 12V voltage is applied to the Gate of both Q3 and Q4. The voltage difference between the Gate and Source, V_{GS} for both Q3 and Q4 is practically 0V. Since both Q3 and Q4 are P-channel MOSFETs, the Drain current is not allowed to flow through (as shown in the transfer characteristic curve in Figure 3.2). The motor is, hence, turned off.

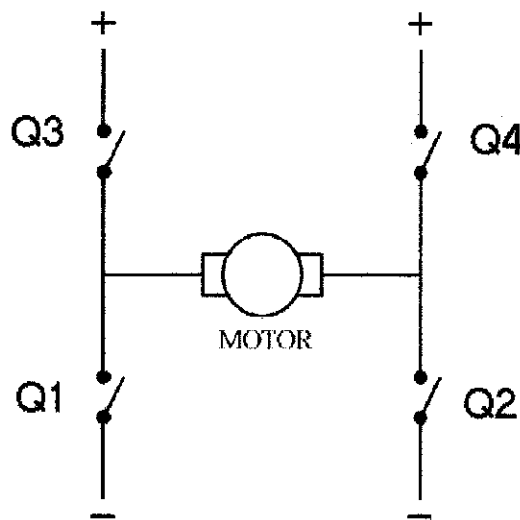


Figure 3.4 Stop Mode

Clockwise and Counterclockwise Mode

When HB-1 is supplied with voltage (eg. 5V) and HB-2 is grounded, HB-1 acts like a closed switch while HB-2 acts like an open switch. In this case, resistors R8 and R7 would form a voltage divider. Due to the great differences between the resistance in R8 and R7, most of the voltage would be consumed by R8; whereas, R7 would only take up a very small portion of the voltage consumption – virtually equivalent to 0V. V_{GS} for Q3 is supplied with voltage while V_{GS} for Q4 remains as 0V.

Since the Base voltage for Q6 (PNP BJT transistor) is almost equivalent to 0V, Q6 is now a closed switch that completes the current flow from the source to R3 and R4 and, eventually, to the ground. R3 and R4 form a voltage divider, whereby; most of the voltage would be consumed by R4, due to its relatively large resistance in comparison with R3. V_{GS} for Q2 would be equivalent to the voltage value in R4. Since Q2 is a N-channel MOSFET, the Drain current is allowed to flow, with the existence of positive voltage in V_{GS} .

Hence, a complete circuit is established, allowing current to flow from the source to Q3, the motor, Q2, and finally to the ground.

The same operational flow applies to the condition whereby HB-2 is supplied with voltage while HB-1 is grounded. Assuming that the motor is turning in clockwise direction in the previous condition (HB-1 = +5V, HB-2 = 0V), it would be turning in the counterclockwise direction in the current condition (HB-1 = 0V, HB-2 = +5V). This is because the polarity of the motor changes in corresponds to the changes in current flow. The changes in the rotational direction of the motor would be able to drive the mobile robot in either the forward or reverse mode.

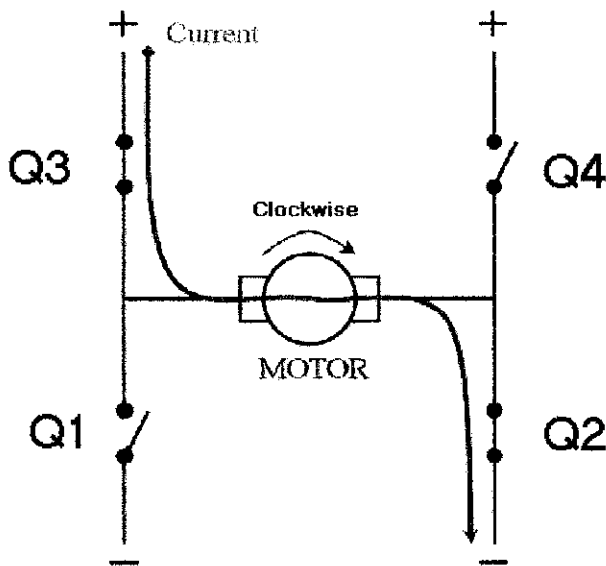


Figure 3.5 Clockwise Direction

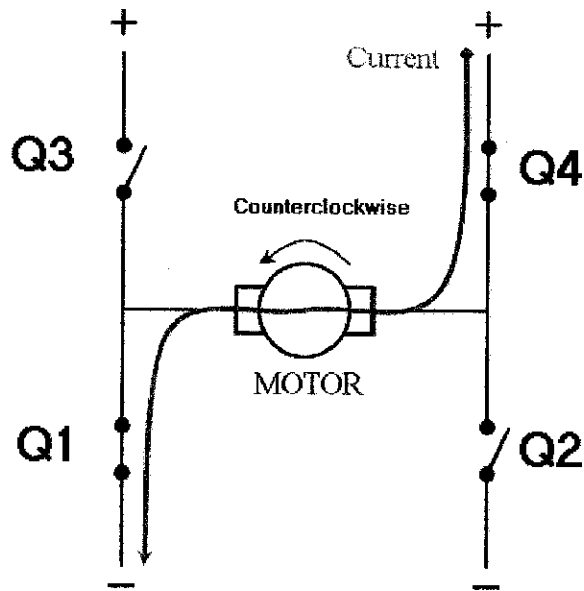


Figure 3.6 Counterclockwise Direction

Not Allowed Mode

Both HB-1 and HB-2 are not allowed to be supplied with voltage at the same time as this would cause a short circuit in the H-bridge circuit. The battery will be shorted out and the H-bridge will literally blow up. This phenomenon is referred to as shoot through.

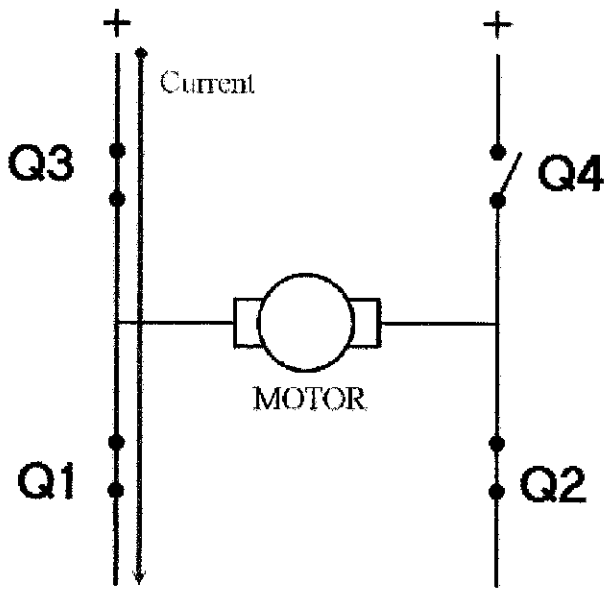


Figure 3.7 Shoot Through Current

3.3 Ultrasonic Sensors

The sensing of an ultrasonic sensor is initiated by first creating a sonic ping at a specific frequency. With a 5V input voltage, the ping is a continuous stream of high-to-low transitions of 0V and 5V. These transitions are usually fed into a transducer at a frequency of around 40kHz or more. For reference, the range of sound capable being captured by a human is between the range of 20Hz to 20kHz. Thus, since the chirp falls out of the hearing range of a human, the chirp is considered inaudible.

The chirp moves radially away from the transducer to the air at approximately 343.2m/s the speed of sound. This speed would be altered by the changes in altitude as it is virtually not affected by pressure. However, it may be slightly affected by the atmosphere humidity. Since the chirp spreads out radially, the signal strength would be attenuated by $1/d^2$ as it travels farther away from the transducer. This means that the maximum distance drops off rapidly at the extreme of maximum of the sensors.

When the ultrasonic chirp bounces into an object, it would be reflected at varying degrees depending on the external shape, orientation, and surface properties of the surface of the object. The reflected chirp would then travel back to the transducer (the receiver) at the speed of the sound. As the reflected chirp reaches the transducer, it is captured and converted to a small voltage signal. The voltage is then fed to a stepped-gain amplifier.

As the signal decreases in strength with distance at an inverse square proportion, the gain of the amplifier is increased exponentially (d^2). This helps to give the best sensitivity across the range of the detector.

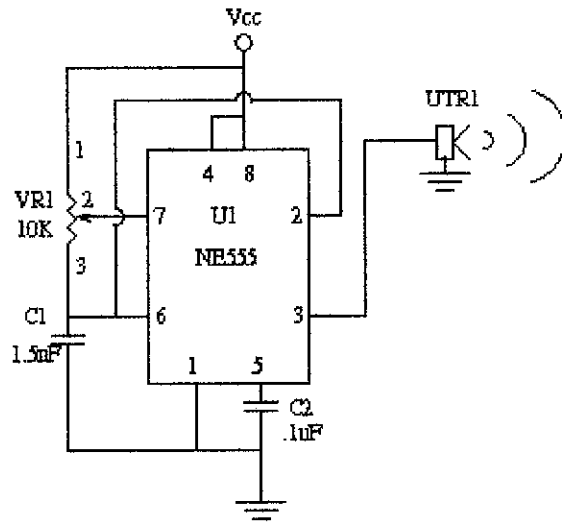


Figure 3.8 Ultrasonic Transmitter

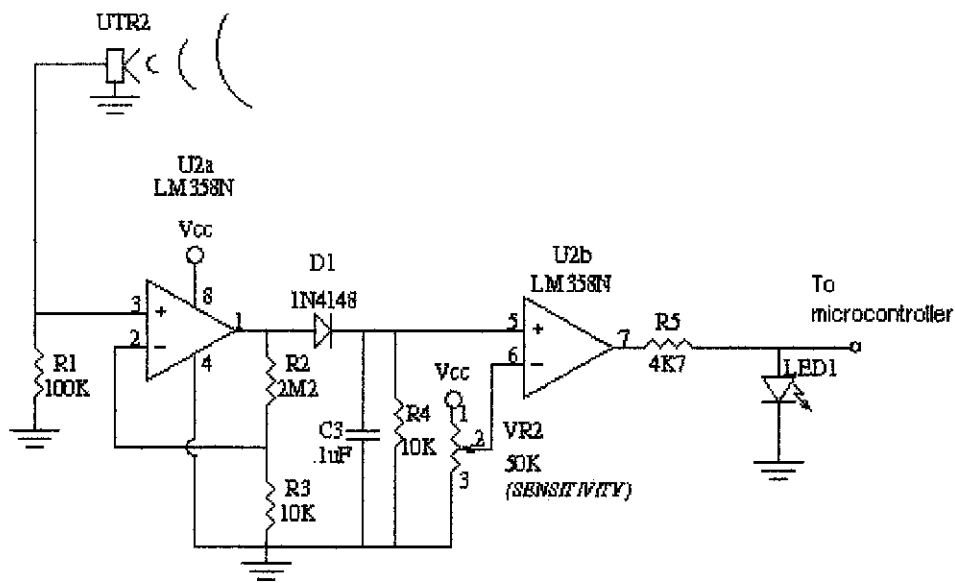


Figure 3.9 Ultrasonic Receiver

3.4 PIC16F84A Microcontroller⁶

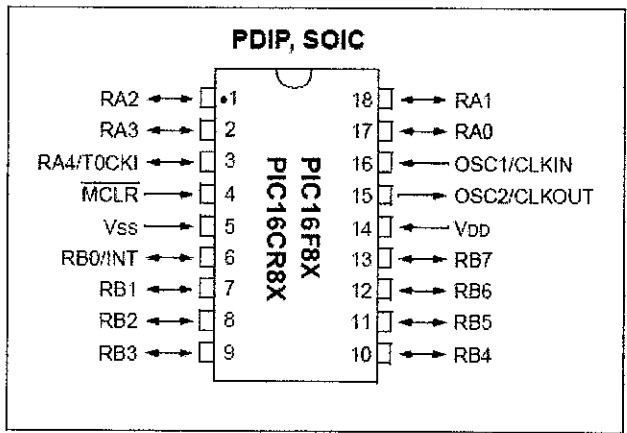


Figure 3.10 The pin diagram of a PIC16F84A microcontroller

Overview

The PIC16F84A chip is placed in a programming unit attached to the host computer for program downloading before fitting it into the target board. The memory in the chip can be reprogrammed without any special erasing process and can be done while the chip is still in the application circuit. The program would also be retained in the chip even when it is disconnected from the power source.

The microcontroller can be considered in 2 parts, the program execution section and the register processing section. Program execution section contains the program memory, instruction register, and control logic, which store, decode and execute the program. The register processing sections has special registers used to set up the processor options, data register to store the current data, port registers for input and output, and ALU to process the data.

The timing and control block coordinates the operation of the 2 parts as determined by the program instructions and responds to external control inputs such as the reset. A maximum frequency is always specified, eg. 10MHz. The PIC16F84A can operate at any frequency below this maximum down to zero. There are 2 ways to stop or redirect a continuous loop which are reset and through interrupt.

source is taken from <http://www.ubasics.com/adam/pic/picprog.html>

ROM Instruction Memory

The PIC16F84A microcontroller consists of 1K words – that is 1024 instructions. The instructions are stored in EEPROM and thus would be almost impossible to be modified.

RAM Memory

The chip consists of a 14 bit program bus and an 8 bit data bus, which are connected to registers, ports, timer, etc. There are 80 RAM locations in the chip where variables are stored. The first 12 RAM locations (\$00 -- \$0B) have internal registers mapped to them. Changing these locations with instructions changes the corresponding registers. These 12 registers are referred to as special function registers. The remaining 68 locations are used for variables and are referred to as general purpose registers.

Banked RAM Memory

There are 5 special function registers that are not among the first 12 address (not even among 80). In order to reach these registers, a bit in the byte at RAM location 3 has to be set. This is called ‘banking’. This location is called STATUS and the bit (bit 5) is called RP0. If RP0 is 0, it is referring to Bank 0; if RP0 is 1, it is referring to Bank 1.

EEPROM Memory

The third type of memory in the PIC16F84A chip is the 64 bytes of reprogrammable memory (8 bit). This is used to hold the values that are to be remembered even after the power is turned off.

CHAPTER 4

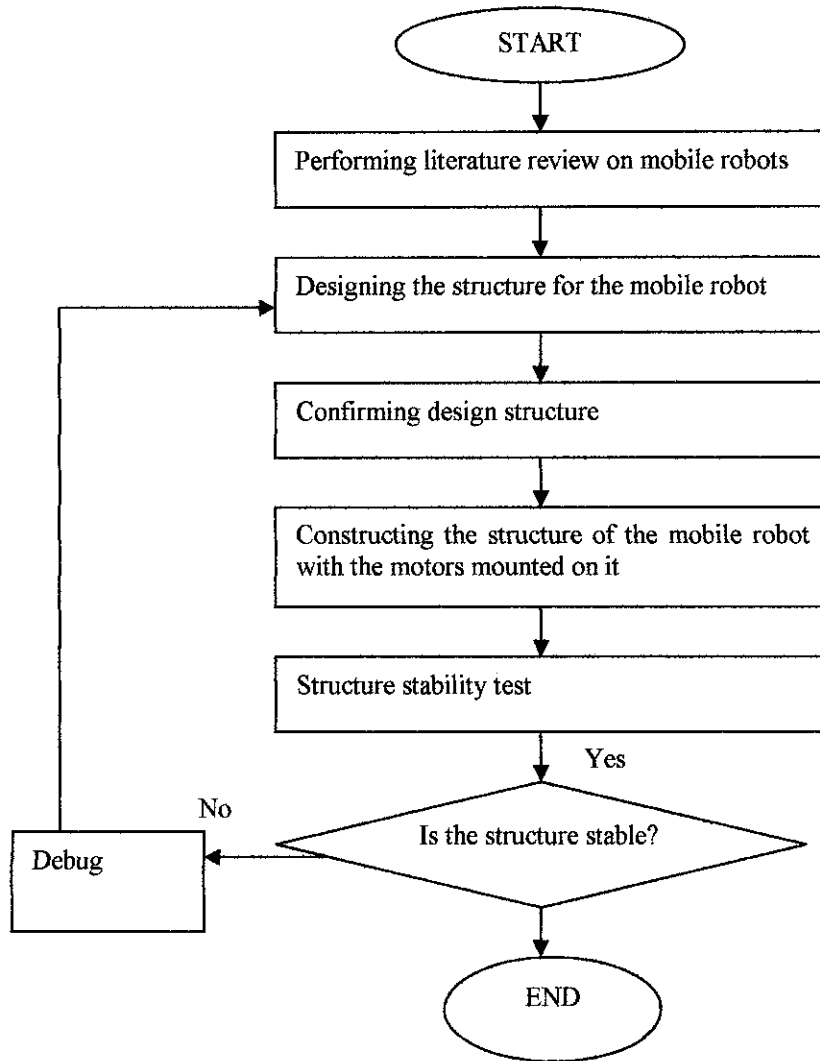
METHODOLOGY/ PROJECT WORK

4.1 Procedure Identification

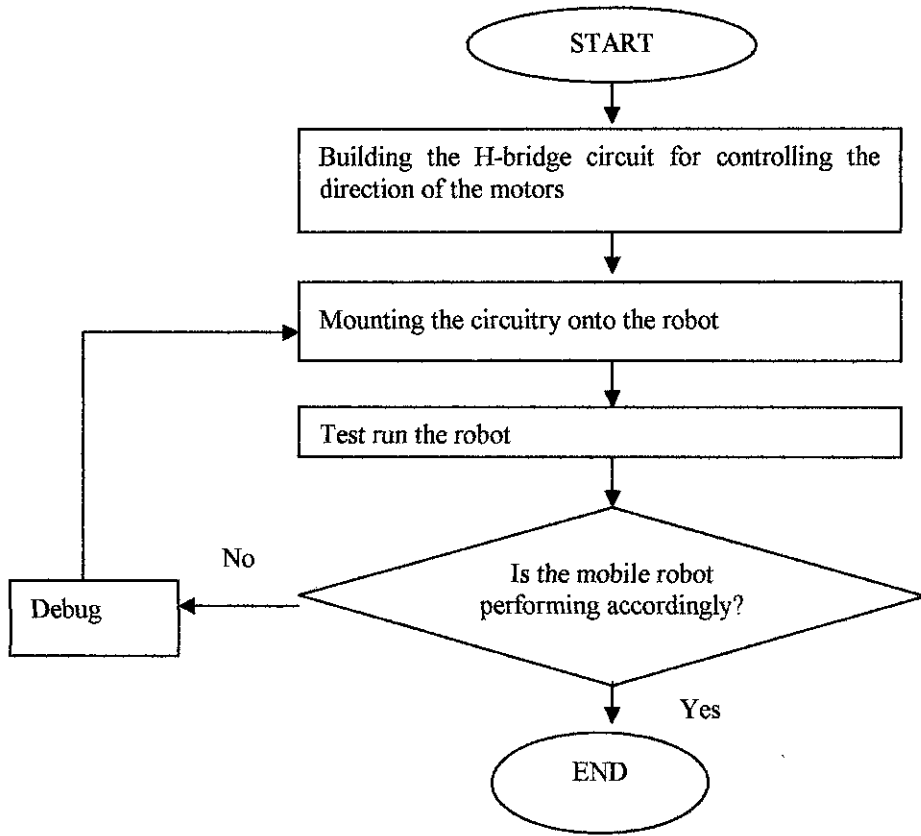
The procedure for building a mobile robot is basically divided into 6 stages:

- (i) Stage 1: Constructing the structure of the mobile robot.
- (ii) Stage 2: Building the circuitry to control the rotational direction of the motors.
- (iii) Stage 3: Programming the PIC16F84A microcontroller for decision-making.
- (iv) Stage 4: Building the ultrasonic sensors circuit.
- (v) Stage 5: Programming path planning algorithm into the PIC16F84A microcontroller.
- (vi) Stage 6: Integrating and validating the end product – the mobile robot.

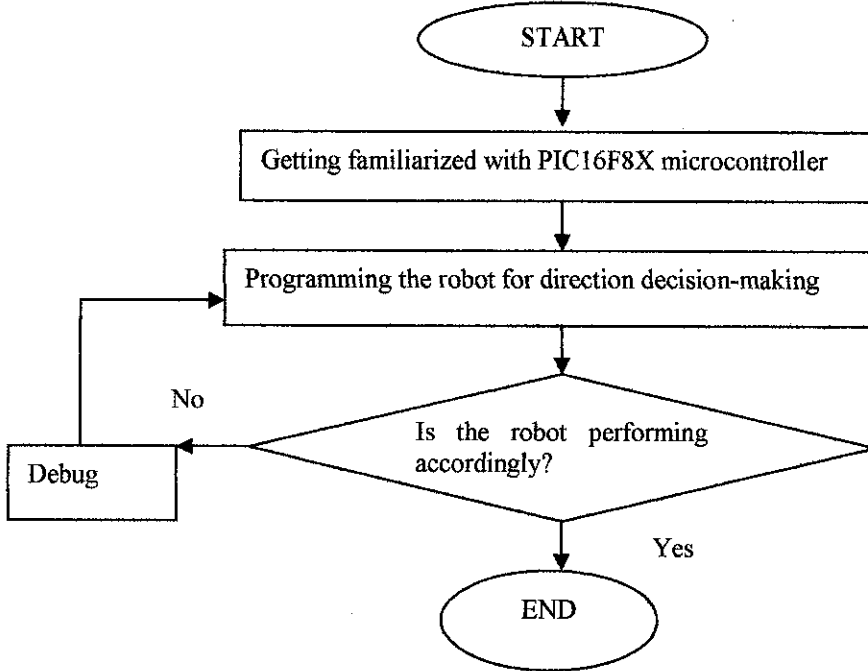
4.1.1 Stage 1: *Building Robot's Structure*



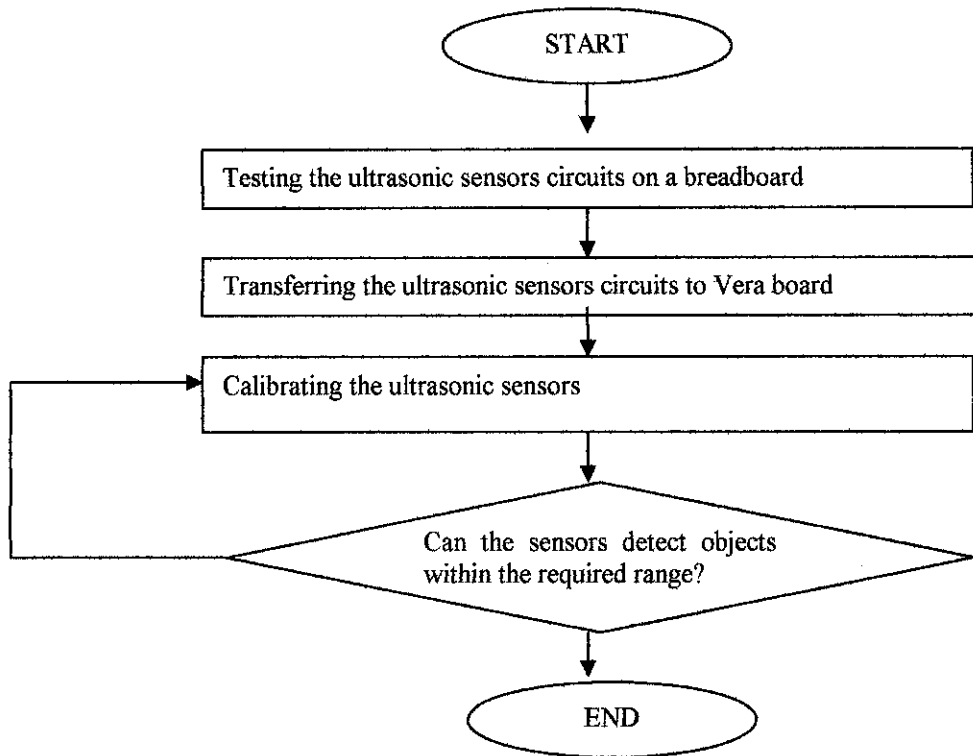
4.1.2 Stage 2: Constructing H-bridge Circuit



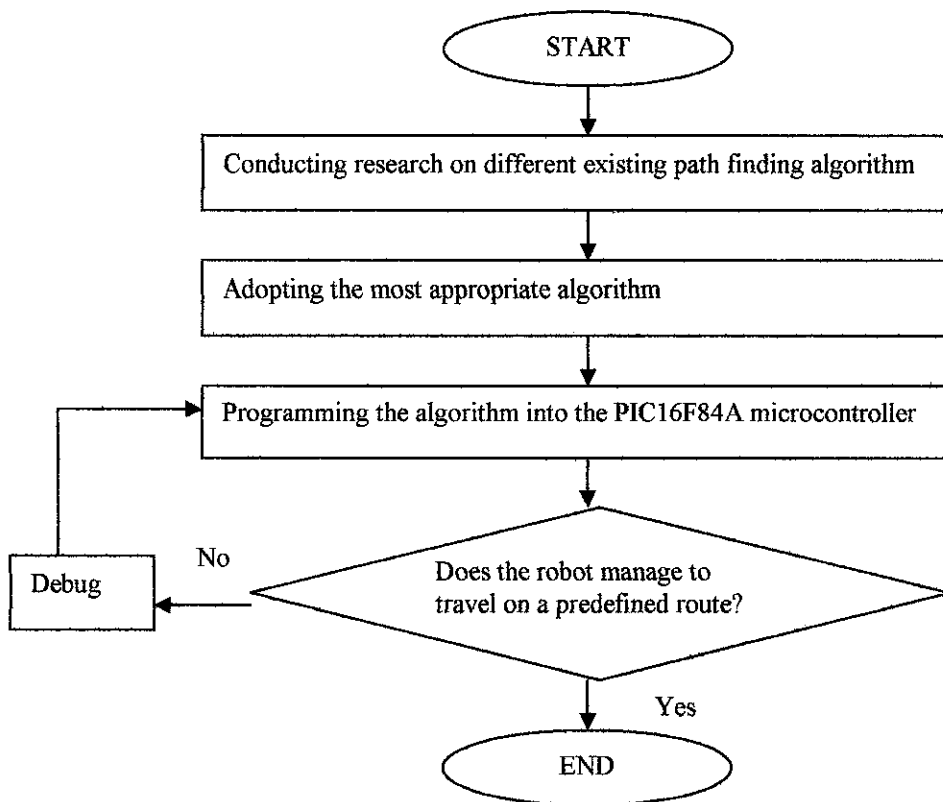
4.1.3 Stage 3: Programming PIC16F84A Microcontroller



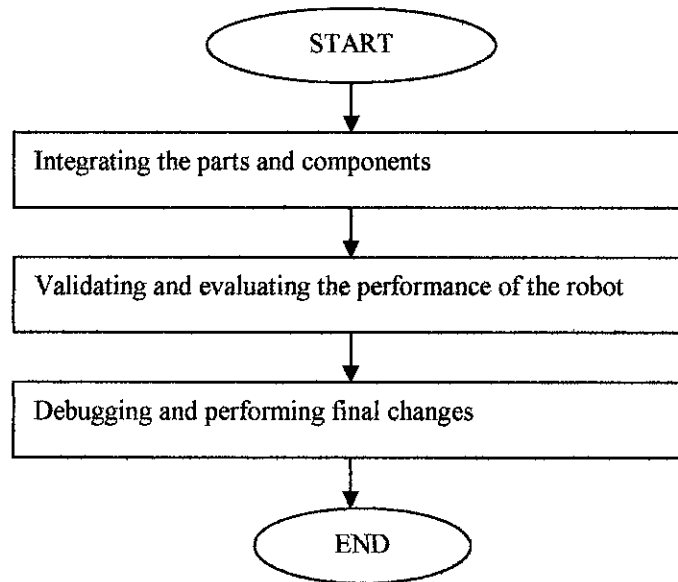
4.1.4 Stage 4: Constructing Ultrasonic Sensors



4.1.5 Stage 5: Programming Path Finding Algorithm



4.1.6 Stage 6: *Integrating and Validating*



4.2 Tools/ Components

- (i) Motors
 - Pittman 9232S001 DC motors
- (ii) Microcontroller
 - PIC16F8X microcontroller
- (iii) Sensors
 - Polaroid Ultrasonic sensors
- (iv) Technical drawing software
 - Microsoft Visio Technical
- (v) Circuitry simulation software
 - Electronic Workbench (EWB)
 - PSPICE
- (vii) Microcontroller Programmer Software
 - MPLAB
 - ICPROG

CHAPTER 5

RESULT AND DISCUSSION

5.1 Structure Design

The diagrams below show the front, side, and bottom view of the mobile robot.

5.1.1 Front View

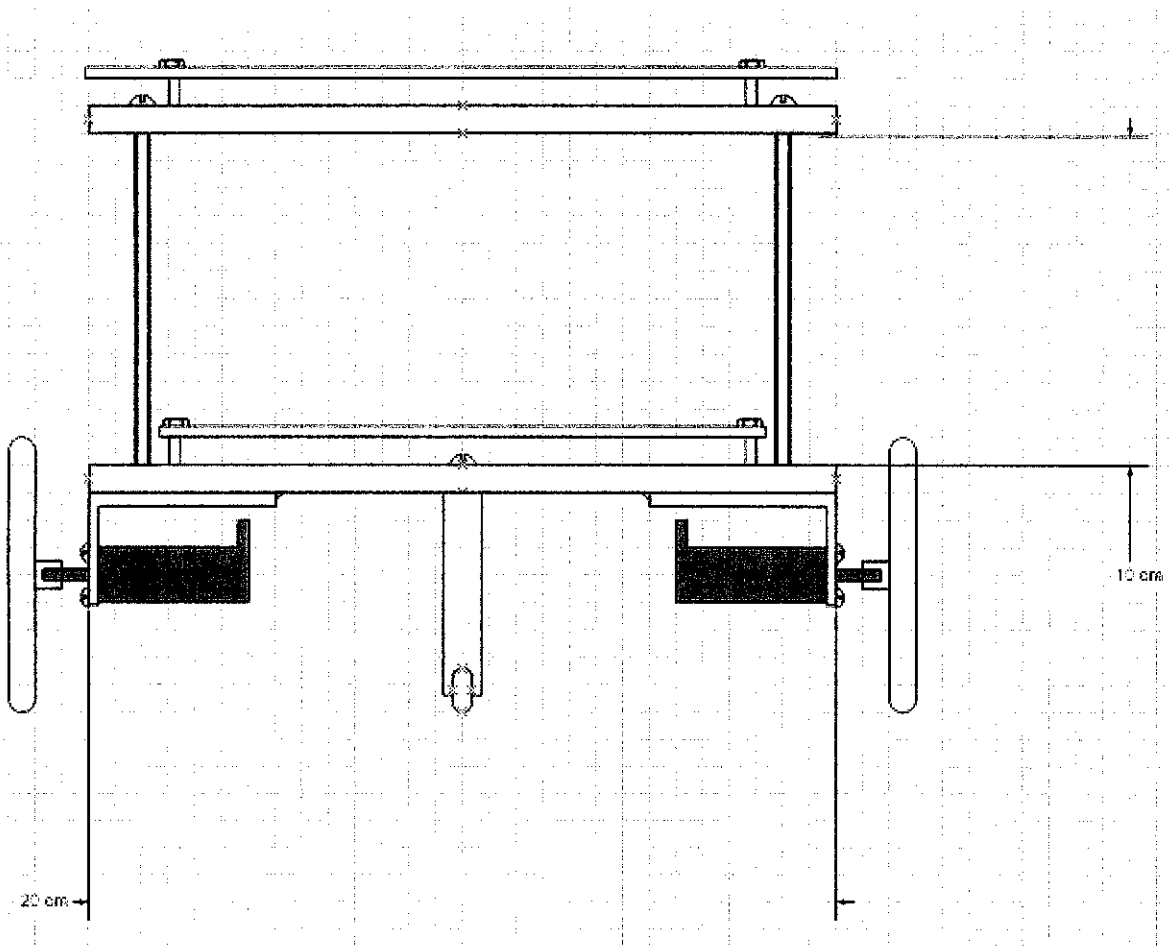


Figure 5.1 Front view of the mobile robot

5.1.2 Side View

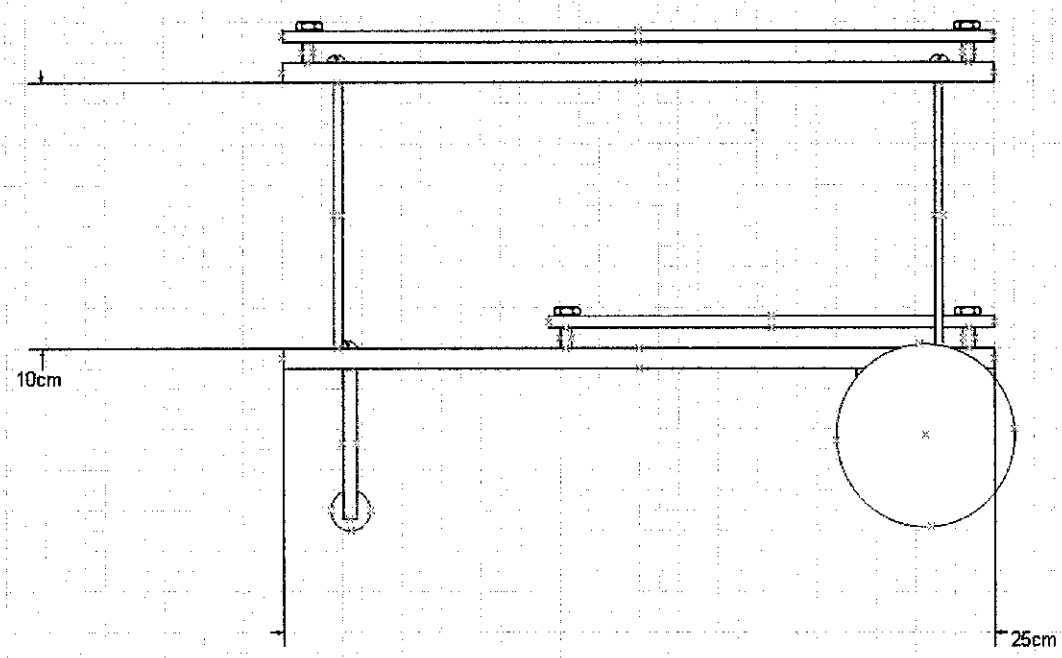


Figure 5.2 Side view of the mobile robot

5.1.3 Bottom View

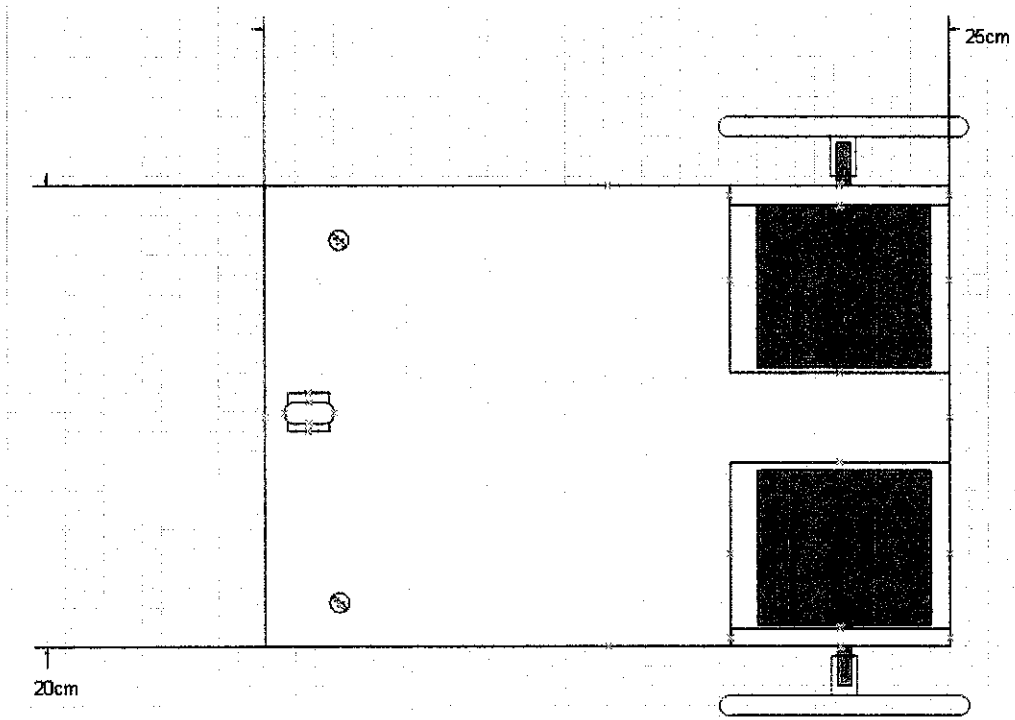


Figure 5.3 Bottom view of the mobile robot

5.1.4 Snap Photos of Overall Design

Below are some of the snap shots of the actual mobile robot:



Figure 5.4 Overall picture of the mobile robot

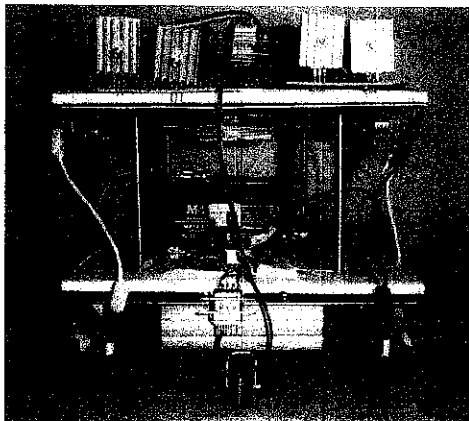
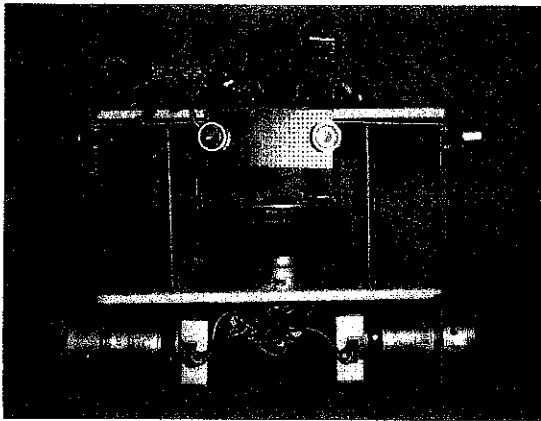


Figure 5.5 Front and back view of the mobile robot

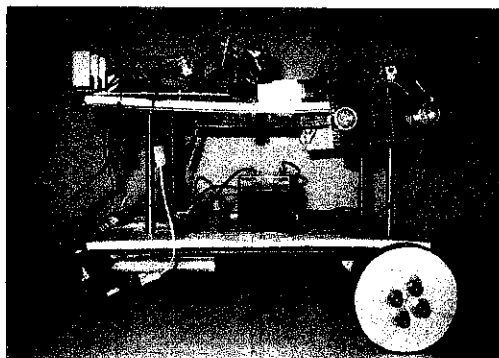


Figure 5.6 Side view of the mobile robot

5.2 H-bridge Circuit in Printed Circuit Board

5.2.1 PSPICE Schematic

The H-bridge circuit is intended to be printed onto a Printed Circuit Board (PCB). The layout of the PCB is drawn using multsim PSPICE software. Thus, a PCPICE schematic is first drawn and is then transferred to the PCB layout using the software.

Figure 5.4 shows the PSPICE schematic for the h-bridge circuit. The 2 Power MOSFETs (MTP3055V and MTP2955V) could not be found in the multsim library, and were, thus, substituted by 2 IRF9140 and IRF150 MOSFETs.

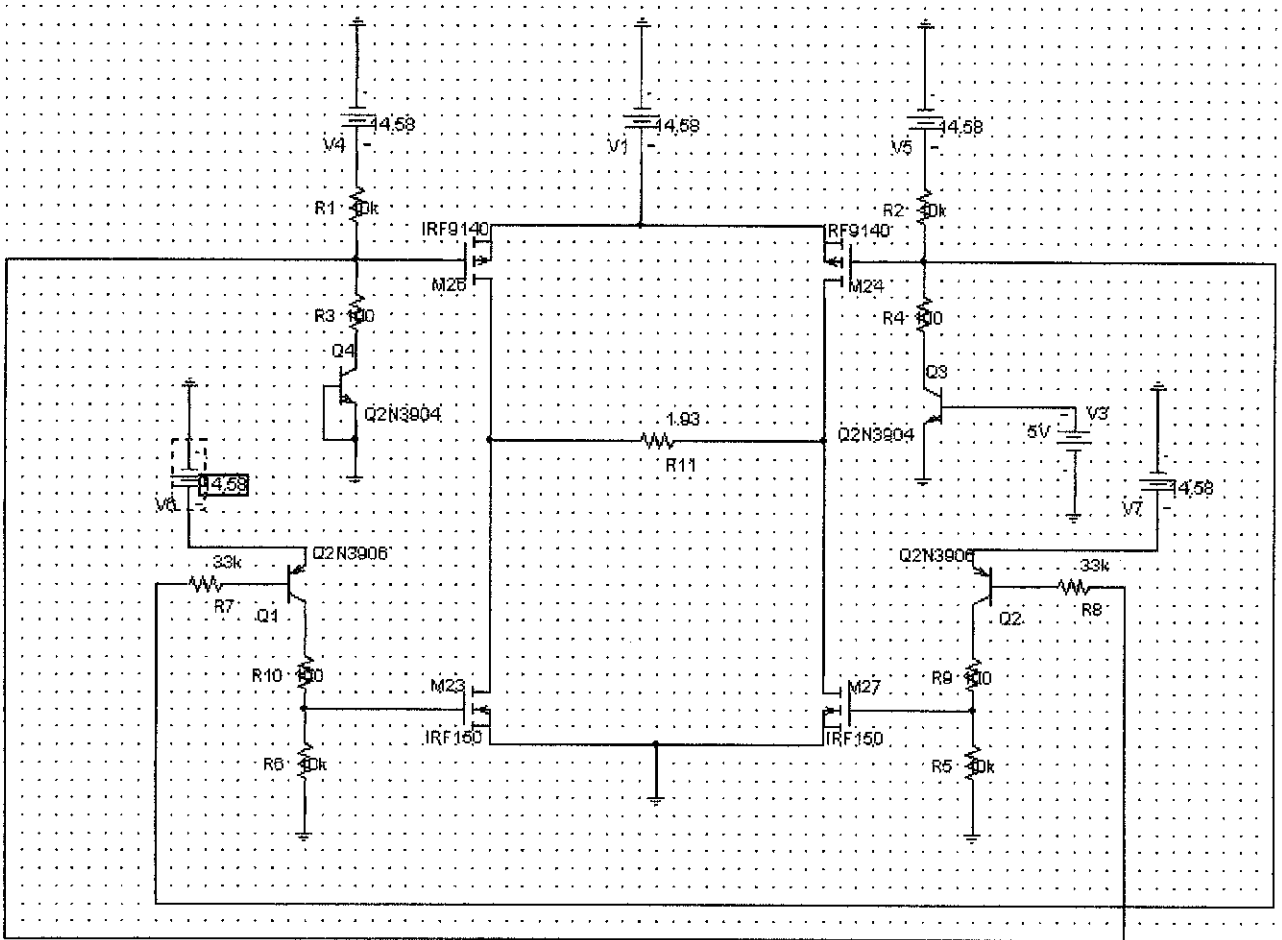


Figure 5.7 H-bridge schematic

5.2.2 PCB Layout

The PCB layout is generated from the PSPICE schematic. Modifications are performed in the multisim PCBoard environment in order to make sure that there are no wires overlapping each other, which may cause short circuit.

Figure 5.5 shows the PCB layout of the h-bridge circuit. The two MOSFETs – MTP2955 and MTP3055 are not found in the multisim PCBoard library. IRF150 and IRF9140 MOSFETs, which are used as a replacement for the above two MOSFETs are found inappropriate either. Thus, 2N3819 transistors are now used as substitutes for the two type MOSFETs (MTP2955 and MTP3055).

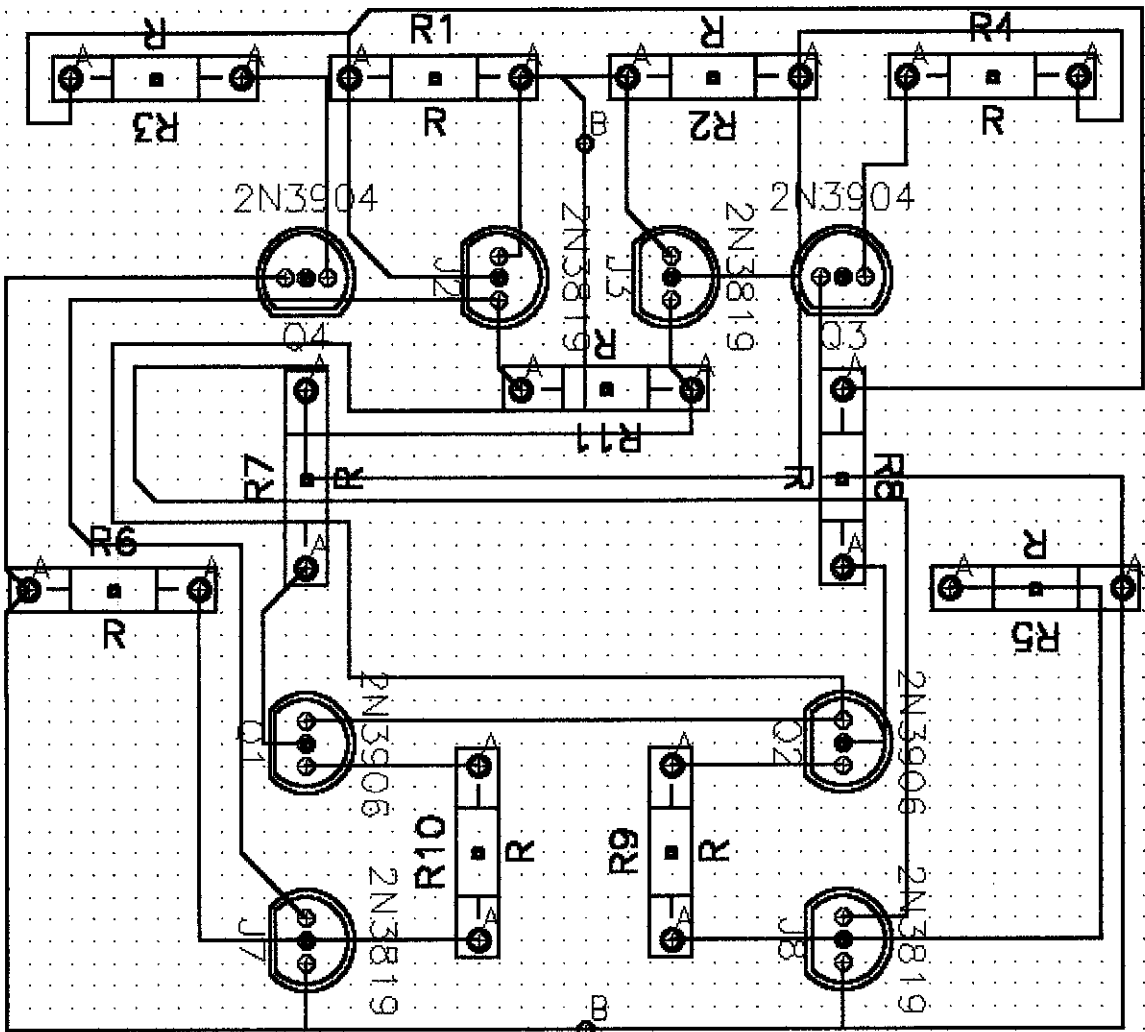


Figure 5.8 PCB layout for the h-bridge circuit

5.3 H-bridge Circuit Calculation

5.3.1 Maximum Torque

The torque of a motor is directly proportional to the current, as given by the equation:

$$\tau_{\text{ind}} = K \Phi I_a$$

where,

τ_{ind} is the induced torque

K is a constant depending on the construction of the machine

Φ is the flux in the machine, which is assumed to be constant

I_a is the armature current in the machine

The peak current is required in order to generate maximum torque to drive the motors. The peak current that could be supported by the 9232S001 model motor is 6.22A. Thus, in order to reach the maximum torque (9.7×10^{-2} Nm) for driving the motor, an approximate of 6A is chosen as the Drain current, I_D .

Thus, for maximum torque

$$\underline{I_D = 6A}$$

P-channel MTP2955 Power MOSFET

For a P-channel MTP2955V Power MOSFET, the following data is given:

Gate-to-source threshold Voltage, $V_{GS(\text{TH})} = 2.8\text{V}$ (typical value)

Drain-to-source Voltage, $V_{DS(\text{ON})} = 2.9\text{V}$

On characteristic Gate-to-source Voltage, $V_{GS(\text{ON})} = 10\text{V}$

On characteristic Drain Current, $I_{D(\text{ON})} = 12\text{A}$

For $V_{GS} > V_{GS(\text{TH})}$ (assuming that both the values are absolute values), the transfer characteristic equation is given by: $I_D = K(V_{GS} - V_{GS(\text{TH})})^2$, where, K is a constant that is a function of the construction of the device. In order to calculate the value of K, the on characteristics value is substituted into the equation.

$$I_D = K (V_{GS} - V_{GS(TH)})^2$$

$$12 = K (10 - 2.8)^2$$

$$\underline{K = 0.2315}$$

The value of Gate-to-source voltage, V_{GS} required obtaining $I_D = 6A$ is:

$$I_D = K (V_{GS} - V_{GS(TH)})^2$$

$$6 = 0.2315 (V_{GS} - 2.8)^2$$

$$\underline{V_{GS} = 7.9V}$$

As shown from the I_D vs V_{DS} graph below (taken from the MTP2955V Power MOSFET datasheet), for $V_{GS} = 8V$ and $I_D = 6A$, $V_{DS} = 1.5V$

$$\underline{V_{DS} = 1.5V}$$

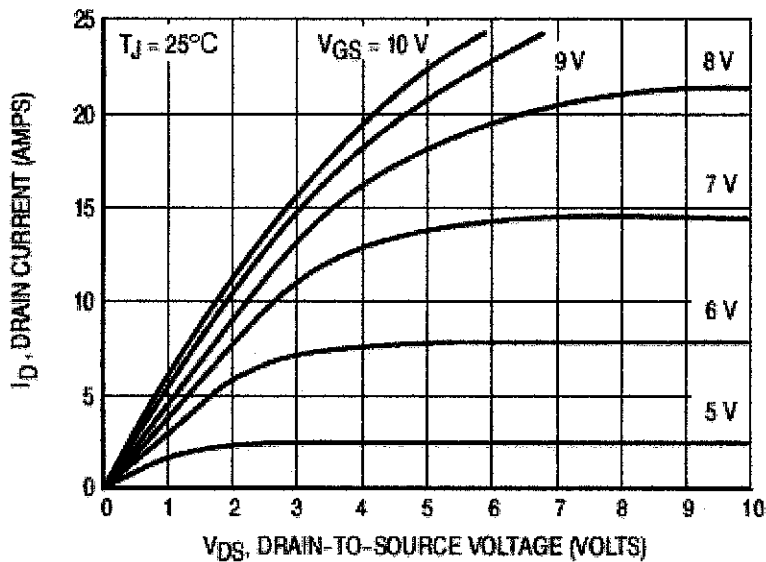


Figure 5.9 On-region characteristic for MTP2955V P-channel Power MOSFET

N-channel MTP3055V Power MOSFET

For an N-channel MTP3055V Power MOSFET, the following data is given:

$$V_{GS(TH)} = 2.7V \text{ (typical)}$$

$$V_{DS(ON)} = 1.3V \text{ (typical)}$$

$$V_{GS(ON)} = 10V$$

$$I_{D(ON)} = 12A$$

In order to calculate the value of K, the on characteristics value is substituted into the equation, $I_D = K (V_{GS} - V_{GS(TH)})^2$.

$$I_D = K (V_{GS} - V_{GS(TH)})^2$$

$$12 = K (10 - 2.7)^2$$

$$\underline{\underline{K = 0.2252}}$$

The value of V_{GS} required to obtain $I_D = 6A$ is:

$$I_D = K (V_{GS} - V_{GS(TH)})^2$$

$$6 = 0.2252 (V_{GS} - 2.7)^2$$

$$\underline{\underline{V_{GS} = 7.9V}}$$

Thus, $V_{GS} = 7.9V$ is required to obtain $I_D = 6A$.

As shown from the I_D vs V_{DS} graph below (taken from the MTP3055V Power MOSFET datasheet), for $V_{GS} = 8V$ and $I_D = 6A$, $V_{DS} = 0.75V$

$$\underline{\underline{V_{DS} = 0.75V}}$$

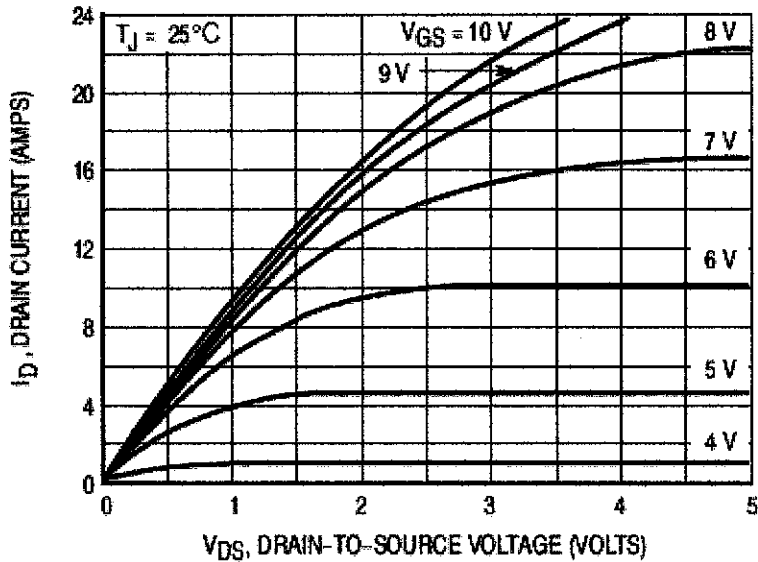


Figure 5.10 On-region characteristic for MTP3055V N-channel Power MOSFET

Hence, the voltage supply, E for the H-bridge circuit is a sum of the Drain-to-source voltage, V_{DS} for P-channel and N-channel and the internal resistance of the motor (found in the data sheet for the 9232S001 model motor):

$$E = V_{DS}(\text{P-channel}) + I_D(R_{\text{motor}}) + V_{DS}(\text{N-channel})$$

$$E = 1.5 + 6(1.93) + 0.75$$

$$\underline{\underline{E = 13.83V}}$$

In short, in order to obtain maximum torque, the following values are required:

$$\mathbf{I_D = 6A}$$

$$\mathbf{V_{GS} \text{ for MTP2955V P-channel} = 7.9V}$$

$$\mathbf{V_{DS} \text{ for MTP2955V P-channel} = 1.5V}$$

$$\mathbf{V_{GS} \text{ for MTP3055V N-channel} = 7.9V}$$

$$\mathbf{V_{DS} \text{ for MTP3055V N-channel} = 0.75V}$$

$$\mathbf{\text{Voltage supply, } E = 13.83V}$$

5.3.2 Normal Torque

The following values are obtained while test running the robot:

Table 5.1 Values measured for I_D and V_{DS}

	I_D in MTP2955V and MTP3055V	V_{DS} in MTP2955V	V_{DS} in MTP3055V	V_{GS} in MTP2955V	V_{GS} in MTP3055V
	2.619A	5.440V	1.213V	4.607V	9.898V
	2.542A	5.109V	1.158V	4.676V	9.973V
	2.706A	4.974V	1.207V	4.653V	9.956V
Average	2.622	5.174	1.193	4.645	9.942

As shown in table 5.1, the sum of both V_{DS} in P channel and N channel is:

$$V_{DS}(\text{P-channel}) + V_{DS}(\text{N-channel}) = 5.174 + 1.193$$

$$\underline{V_{DS}(\text{P-channel}) + V_{DS}(\text{N-channel}) = 6.367V}$$

Given:

$$E = V_{DS}(\text{P-channel}) + I_D(R_{\text{motor}}) + V_{DS}(\text{N-channel})$$

A 12V gell cell battery is used as the power supply. Thus, E measured = 12.496V

The internal resistance of the DC motor = 1.93Ω

Hence, the calculated values for $V_{DS}(\text{P-channel}) + V_{DS}(\text{N-channel})$ is:

$$12.496 = V_{DS}(\text{P-channel}) + 2.56(1.93) + V_{DS}(\text{N-channel})$$

$$12.496 = V_{DS}(\text{P-channel}) + V_{DS}(\text{N-channel}) + 4.94$$

$$\underline{V_{DS}(\text{P-channel}) + V_{DS}(\text{N-channel}) = 7.556V}$$

5.3.3 The Effect of Loads on I_D , V_{GS} , and V_{DS}

Different loads are put onto the mobile robot in order to measure and analyze the effect of loads on the I_D , V_{GS} , and V_{DS} of the MOSFETs in the H-bridge circuit. 3 different weights are selected for the loads. They are 500g, 1000g, and 1500g respectively.

Table 5.2 shows the result obtained for the three different loads tested. The net weight for the mobile robot is 3.5kg. The graphs for I_D vs load, V_{GS} vs load, and V_{DS} vs load are also shown.

Table 5.2 Result for I_D , V_{GS} , and V_{DS} in different loads

Total Weight	Load	I_D for both P and N channel MOSFET	V_{GS} for P-channel MOSFET	V_{DS} for P-channel MOSFET	V_{GS} for N-channel MOSFET	V_{DS} for N-channel MOSFET
3.5kg	0.0kg	2.302A	4.379V	5.264V	9.817V	1.113V
4.0kg	0.5kg	2.353A	4.498V	5.560V	9.895V	1.143V
4.5kg	1.0kg	2.482A	4.589V	5.633V	10.116V	1.207V
5.0kg	1.5kg	2.687A	4.633V	5.687V	10.317V	1.262V

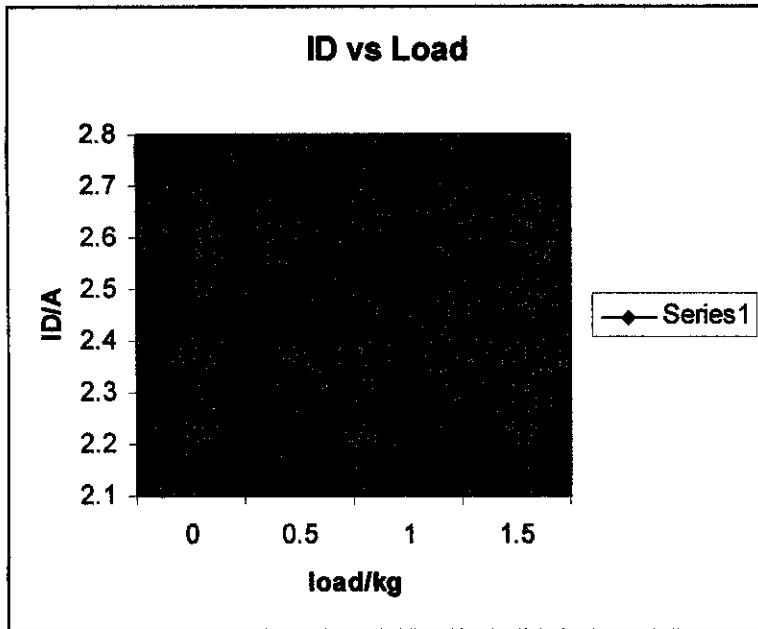


Figure 5.11 I_D vs Load

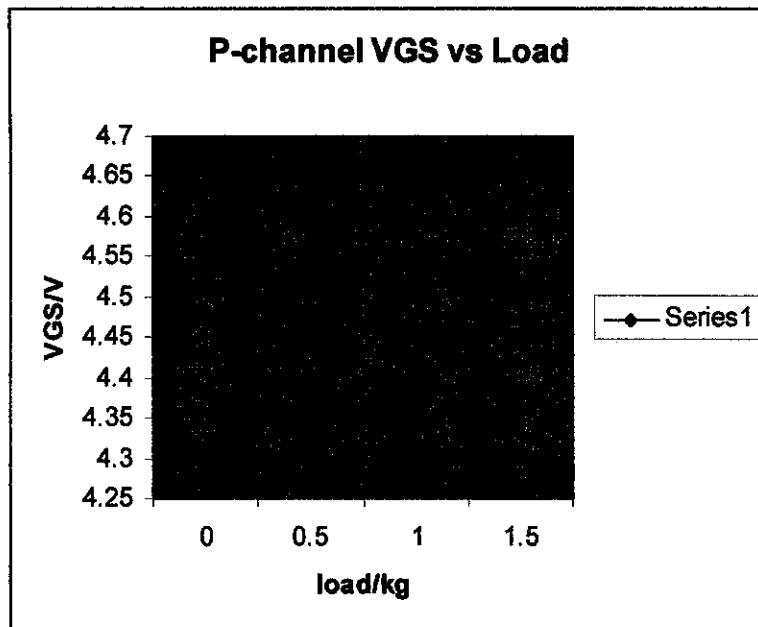


Figure 5.12 P-channel V_{GS} vs Load

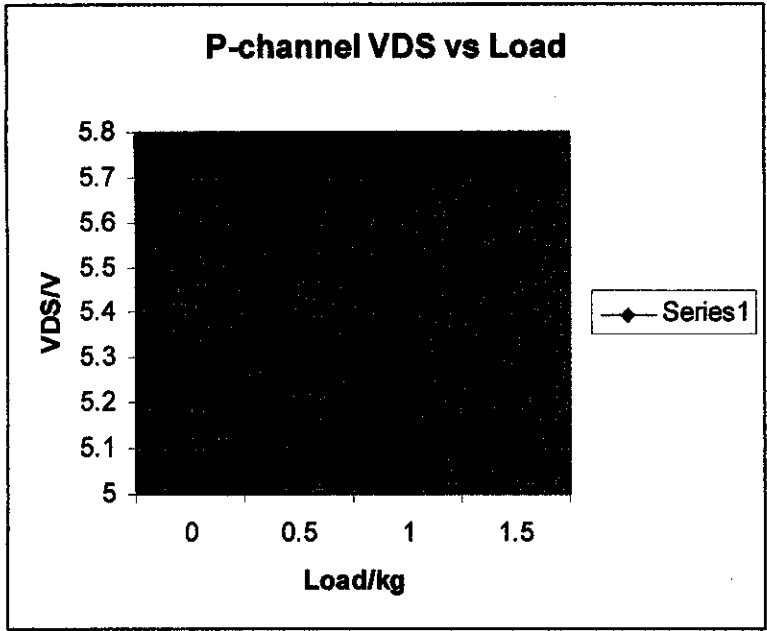


Figure 5.13 P-channel V_{DS} vs Load

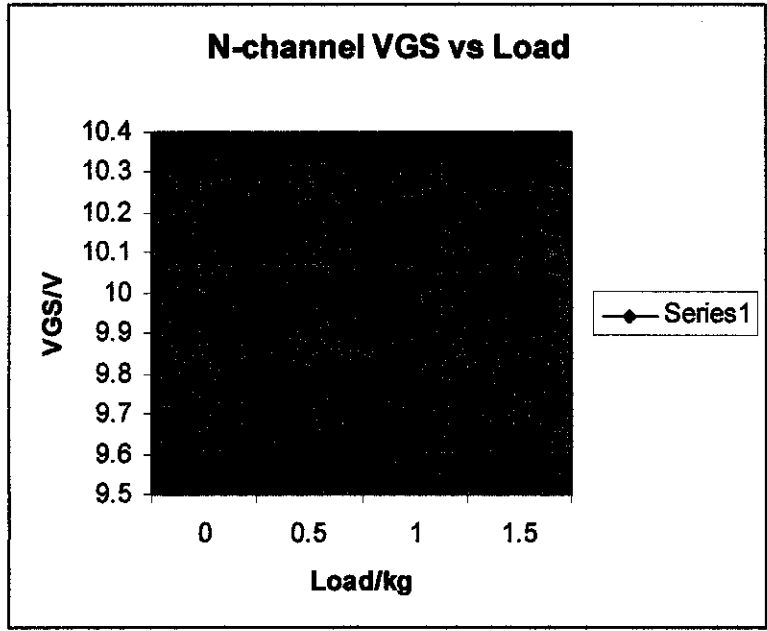


Figure 5.14 N-channel V_{GS} vs Load

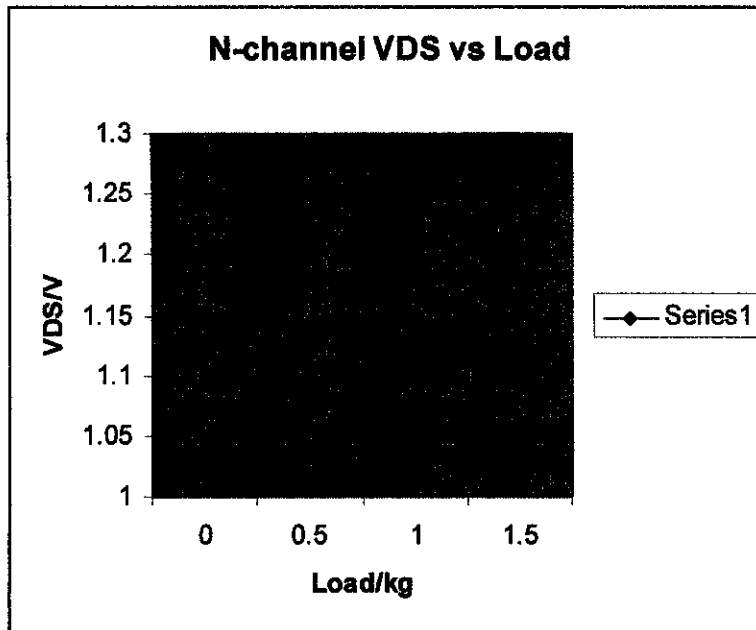


Figure 5.15 N-channel VDS vs Load

5.3.4 Discussion

An Analysis on Maximum and Normal Torque Performance

According to the datasheet of the 9232s001 Pittman dc motor, the peak current that can be supported by the motor is 6.22A. Thus, as a safety measurement, the motor should always operate at no more than 6A. As shown from the calculation in 5.3.1, in order not to allow the current from exceeding its maximum allowable limit, the maximum voltage supplied to the h-bridge should never be more than 13.83V.

Section 5.3.2 shows the values of I_D , V_{DS} and V_{GS} for both MTP2955V and MTP3055V MOSFETs. By using a power supply of 12V, it is obvious that the average current supplied to the h-bridge circuit and the motor is not more than half of the peak current. Thus, this implies that the motor would never reach its maximum torque at normal operating condition. Also, this elude the possibility that the current drawn to the motor may exceed its maximum limit, thus, damaging the motor.

Section 5.3.2 also proved that the sum of both V_{DS} measured in both MTP2955V P-channel MOSFET and MTP3055V N-channel MOSFET differ slightly with the sum value calculated. The difference may be due to the variation in the current drawn by the motors.

It can be seen that the characteristic of V_{DS} and V_{GS} for MTP2955V MOSFET (as shown in table 5.1) complies with the on region characteristic graph for MTP2955V MOSFET (Figure 5.9). However, the characteristic of V_{DS} and V_{GS} for MTP3055V MOSFETs (as shown in table 5.1) does not obey the on-region characteristic graph of MTP3055V (Figure 5.10). Figure 5.10 shows that, with $V_{DS} = 1.193V$ and $V_{GS} = 9.942V$, the Drain current, I_D , should exceed 8A. However, the value of I_D measured above merely has an average value of 2.622A. This may be because I_D flowing from the motor to the Drain pin of the MTP3055V N-channel MOSFET is restricted by the Drain current flowing from the MTP2955V P-channel MOSFET to the motor.

An Analysis on the Effect of Loads on an H-bridge Circuit

As can be seen in Figure 5.11, the value of I_D (which is the current flowing through the 2 MOSFETs and the motor) increases with the increase of loads. This is because when the load on the robot increases, the load torque, τ_{load} exceeds the induced torque, τ_{ind} and the speed of the motor, ω tends to slow down. When the speed of the motor slows down, its internal generated voltage (the voltage supplied to the rotor of the motor), E_A drops as well. The relationship between the speed of the motor and its internal generated voltage is given by $E_A = K \Phi \omega$; whereby,

E_A is the internal generated voltage

K is a constant depending on the construction of the machine

Φ is the flux in the machine, which is assumed to be constant

ω is the speed of the machine's rotor

The armature current of a dc motor, I_A is given by $I_A = (V_T - E_A)/R_A$; whereby,

I_A is the armature current

V_T is the supply voltage to the motor

E_A is the internal generated voltage

R_A is the total resistance in the entire rotor structure

Thus, when the internal generated voltage, E_A decreases, the armature current will increase. Apparently, with an increase in the armature current, the total current supplied to the dc motor shall increase as well.

The rise of the armature current allows the induced torque, τ_{ind} to increase. This can be shown in the relationship between τ_{ind} and I_A : $\tau_{ind} = K \Phi I_a$. Eventually, the induced torque will rise to a level equivalent to the load torque, τ_{load} with a lower mechanical speed.

It is observed that, the voltage values for both V_{GS} and V_{DS} in both P channel and N channel also increase with the increase of loads. This phenomenon complies with the transfer characteristic curve of a MOSFET. As shown in **Figure 3.2**, V_{GS} will rise as the drain current, I_D (that is, the current flowing through the MOSFETs and the dc motor) increases.

As shown in **Figure 5.9**, the on-region characteristic curve for both P-channel MOSFET proves that the increase of I_D and V_{GS} will cause the voltage value in V_{DS} to increase. Similarly, **Figure 5.10** also shows that the same concept applies to an N-channel MOSFET – that is, an increase in I_D and V_{GS} will result in an increase in V_{DS} .

5.4 Ultrasonic Sensors

5.4.1 Transmitter

The frequency of the ultrasonic chirp being transmitted would be calculated.

The equation for calculating the frequency of a pulse being transmitted from a 555 timer is given below:

1.44

Frequency, $f = \frac{1.44}{(R_1 + 2R_2) C_1}$

$$(R_1 + 2R_2) C_1$$

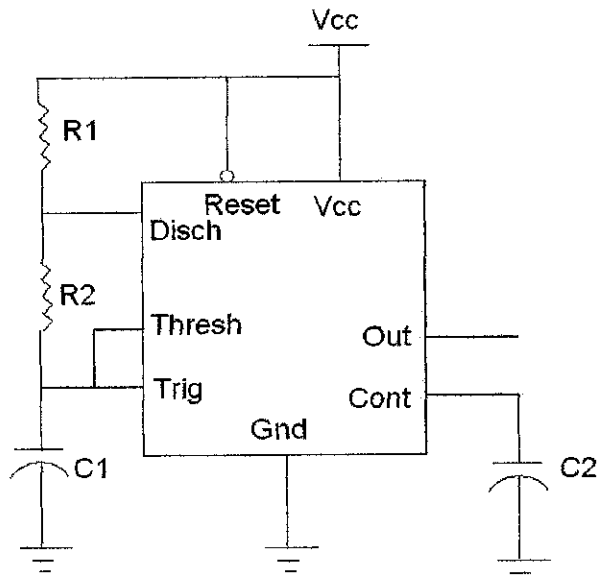


Figure 5.16 A 555 timer diagram

The values for R_1 , R_2 , and C_1 are:

$$R_1 = 1.2\text{k}\Omega$$

$$R_2 = 8.8\text{k}\Omega$$

$$C_1 = 1.5\text{nF}$$

1.44

$$f = \frac{1}{\text{period}}$$

$$[1.2k + 2(8.8k)]1.5n$$

$$f = 51.06\text{kHz}$$

Thus, the calculated value for the frequency of the ultrasonic transmitter is 51.06kHz

The pulse of the ultrasonic transmitter is measured using an oscilloscope. The waveform is observed and a sketch is drawn below:

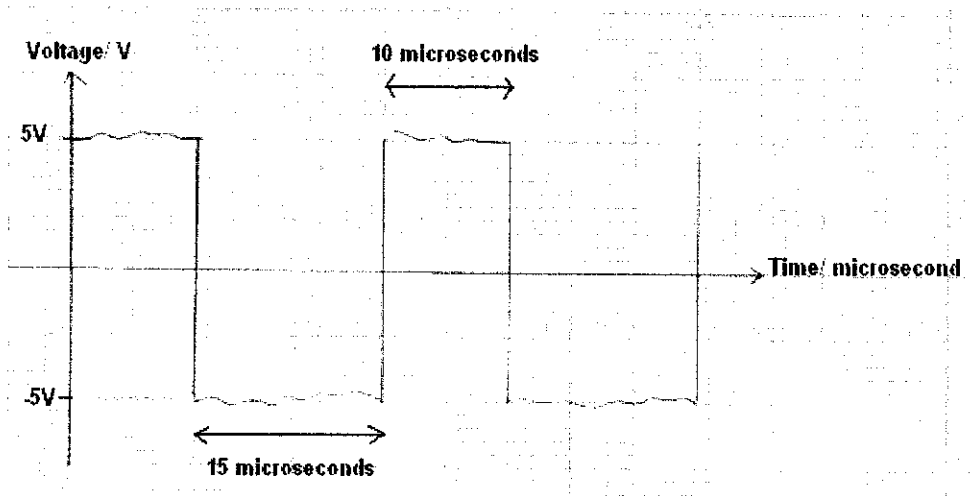


Figure 5.17 Waveform from a 400st ultrasonic transmitter

As can be seen, the period of a cycle is approximately 25 μ seconds.

$$\text{Frequency, } f = 1/\text{period}$$

$$f = 1/(25\mu)$$

$$f = 40\text{kHz}$$

Thus, the measured value for the frequency of the ultrasonic transmitter is 40kHz

5.4.2 Receiver

The closed-loop gain of the operational amplifier, U2a, and the voltage divider in U2b would be calculated.

The configuration used for the U2a op-amp in the receiver circuit is a non-inverting amplifier.

The equation of the closed-loop gain for a non-inverting amplifier configuration op-amp is given as:

$$A = \frac{V_{out}}{V_{in}} = 1 + \frac{R_f}{R_i}$$

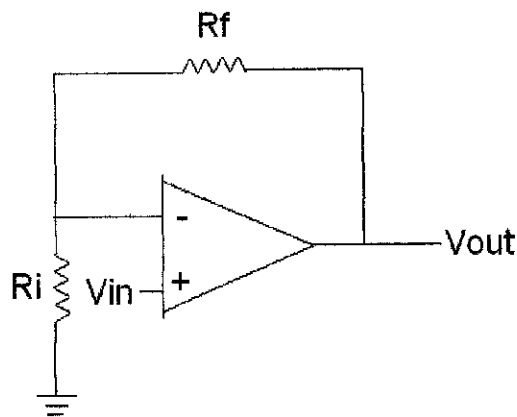


Figure 5.18 Non-inverting Amplifier

The values of R_2 and R_3 of U2a (as shown in Figure 3.9) are:

$$R_2 = 2.2 \text{ M}\Omega$$

$$R_3 = 10 \text{ k}\Omega$$

The closed-loop gain of U2a is

$$2.2 \times 10^6$$

$$A = 1 + \frac{\text{-----}}{\text{-----}}$$

$$10 \times 10^3$$

$$\underline{\underline{A = 221}}$$

Thus, the closed-loop gain for U2a op-amp = 221

An obstacle is put opposite the ultrasonic sensor at different distances. The reflected waveforms from different distances are captured by the ultrasonic receiver. The reflected waveforms are observed to be in sinusoidal form and their amplitude voltages ($V_{in(p)}$) are recorded.

The amplitude of the output voltage ($V_{out(p)}$) is calculated using the following equation:

$$V_{out(p)} = A (V_{in(p)})$$

Table 5.3 shows the peak input voltages and their respective amplified peak output voltages at U2a op-amp. Data is taken at various distances between the obstacle and the ultrasonic sensor:

Table 5.3 $V_{in(p)}$ versus $V_{out(p)}$ calculated and $V_{out(p)}$ measured

Distance	$V_{in(p)}$	$V_{out(p)}$ Calculated	$V_{out(p)}$ Measured
2 cm	3.5 mV	0.77V	0.68V
4 cm	3.6 mV	0.80V	0.68V
6 cm	3.5 mV	0.77V	0.68V
8 cm	3.5 mV	0.77V	0.68V
10 cm	3.4 mV	0.75V	0.68V

12 cm	3.4 mV	0.75V	0.68V
14 cm	3.2 mV	0.71V	0.68V
16 cm	3.2 mV	0.71V	0.60V
18 cm	2.8 mV	0.62V	0.56V
20 cm	2.6 mV	0.57V	0.56V
22 cm	2.6 mV	0.57V	0.56V
24 cm	2.6 mV	0.57V	0.56V
26 cm	2.0 mV	0.44V	0.48V
28 cm	2.0 mV	0.44V	0.48V
30 cm	1.7 mV	0.38V	0.48V
32 cm	1.6 mV	0.35V	0.40V

Figure 5.18 shows a plot of the measured amplified output voltage $V_{out(p)}$ for U2a op-amp versus the increase in distance between the obstacle and the ultrasonic circuit.

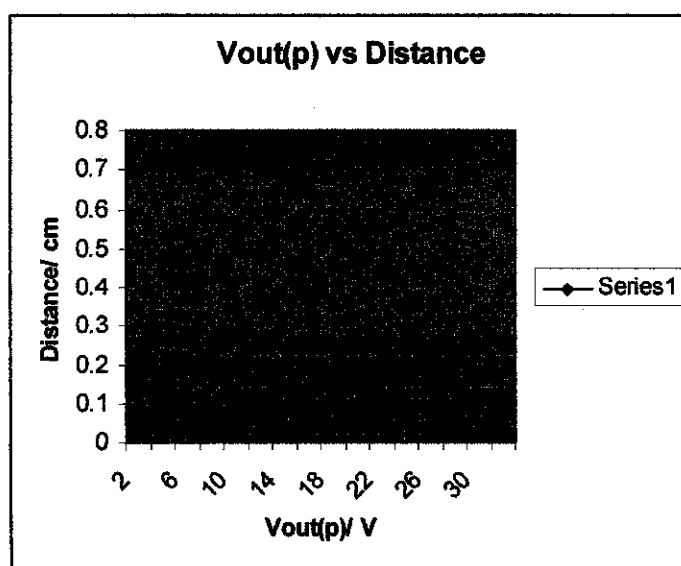


Figure 5.19 A plot of the measured values of $V_{out(p)}$ versus distance.

The configuration used in the U2b op-amp is a comparator circuit.

The circuit connected to the inverted input of U2b is a voltage divider and the reference voltage supplied into U2b is given by the equation below:

$$V_{ref} = \frac{R_2}{R_1 + R_2} (V_{cc})$$

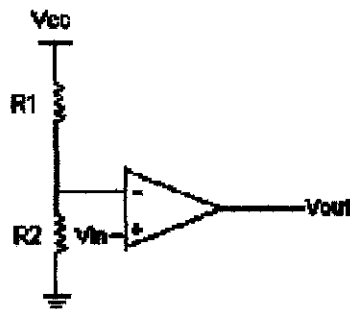


Figure 5.20 Op-amp used as a comparator

A rheostat is used to adjust the ratio of resistance between Vcc to VR2 and VR2 to Gnd.

The resistance from VR2 to Gnd = 3kΩ

The resistance of VR2 = 50kΩ

$$V_{ref} = \frac{3k}{50k} (5)$$

Vref = 0.3V

Table 2 shows a summary of the calculated and the measured values of Vref:

Table 5.4 Reference Voltage

	Calculated	Measured
Vref	0.3V	0.4V

5.4.3 Discussion

As can be seen in **Figure 3.8** the transmitter circuit consists of a 555 timer. The purpose of the 555 timer is to generate pulses such that the transducer is able to transmit ultrasonic chirp at a specified interval. It is noticed that the calculated frequency differs with the actual frequency measured using an oscilloscope. This is because the ultrasonic transducer used here is a pair of 400st and 400sr transmitter and receiver respectively. The transducer can only allow a maximum frequency of up to 40kHz.

The receiver circuit comprises 2 main components – the U2a op-amp and U2b op-amp. U2a is a non-inverting amplifier. The function of U2a is to amplify the voltage signal received from the ultrasonic receiver as it may seem too small to be detected. The output of U2a is then connected to the non-inverting input of U2b. U2b basically forms a comparator circuit. The inverting input of U2b is connected to a voltage divider. The voltage divider provides a reference voltage to the op-amp. The output of U2b stays at a high voltage level (5V) when the non-inverting input is greater than the inverting input and switches to a low voltage level (0V) when the non-inverting input voltage goes below the inverting voltage.

There are certain discrepancies between both the values being calculated and measured in $V_{out(p)}$. However, the differences are considered acceptable. This is because tolerance exists in the devices (such as the op-amp, the oscilloscope, and the multimeter) used. The values measured from the voltage output of the U2a op-amp differs from the value calculated may also be due to the instability voltage supply from the ultrasonic receiver. This is because the reflected signal captured by the ultrasonic receiver is not constant and is always fluctuating depending on the properties of the surfaces the ultrasonic pulse hits.

Also, it is observed that $V_{out(p)}$ from U2a drops gradually when the distance between the obstacle and the ultrasonic sensor increases. When the distance exceeds 32cm, $V_{out(p)}$

basically drops to an amplitude voltage of less than 0.4V. Since the reference voltage for the comparator circuit in U2b op-amp is 0.4V (the measured value is taken into consideration), when $V_{out(p)}$ from U2a goes below 0.4V, basically no voltage could be detected from the output of the comparator circuit. Hence, the ultrasonic sensor will assume no obstacle when the obstacle is more than 32cm away from the mobile robot.

5.5 Features of the Mobile Robot

The mobile robot consists of 2 different features -- that is:

- (i) Obstacle Avoidance
- (ii) Path Finding

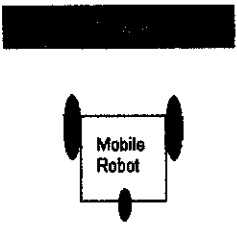
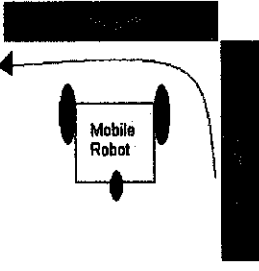
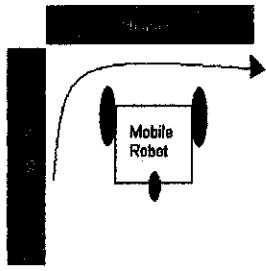
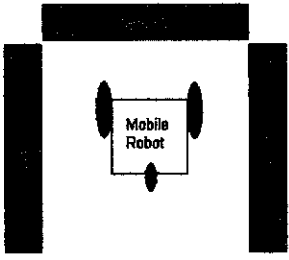
A switch in port B pin 6 is used to determine if the robot is to perform obstacle avoidance or navigate on a predetermined route programmed within the microcontroller. When the switch is off, the mobile robot will avoid all obstacles detected while moving freely. However, when the switch is on, the mobile robot will maneuver on a fixed path preprogrammed into its microcontroller.

5.5.1 Obstacle Avoidance

Several situations have to be taken into consideration while programming the robot to avoid obstacles. The mobile robot should be able to identify the direction of the obstacles, and to decide on the direction it should turn in order to avoid from encumbering with those obstacles.

Some of the situations the mobile robot may encounter and the turning decisions it should take is categorized in **Table 5.5**.

Table 5.5 Decisions taken by the mobile robot at different situations

Case	Obstacles Detected	Decision
<p>Case 1:</p> 	<p>Only front obstacle are detected.</p>	<p>Mobile robot stops.</p>
<p>Case 2:</p> 	<p>Front and right obstacles are detected.</p>	<p>Mobile robot turns left.</p>
<p>Case 3:</p> 	<p>Front and left obstacles are detected.</p>	<p>Mobile robot turns right.</p>
<p>Case 4:</p> 	<p>Front, left, and right are obstacles detected.</p>	<p>Mobile robot stops.</p>

5.5.2 Path Finding

When the switch at port B pin 6 of the PIC16F84A microcontroller is on, the mobile robot is prepared to maneuver on a preprogrammed path. Nevertheless, the robot would still perform obstacle avoidance as in case 2, 3, and 4 shown in table 5.5. The preprogrammed path would only be executed when the robot detects an obstacle at its front (as in case 1 in table 5.5).

The path designed for the mobile robot is a simple one and it is divided into 4 stages (labeled as 1, 2, 3, and 4) as shown in **Figure 5.20**.

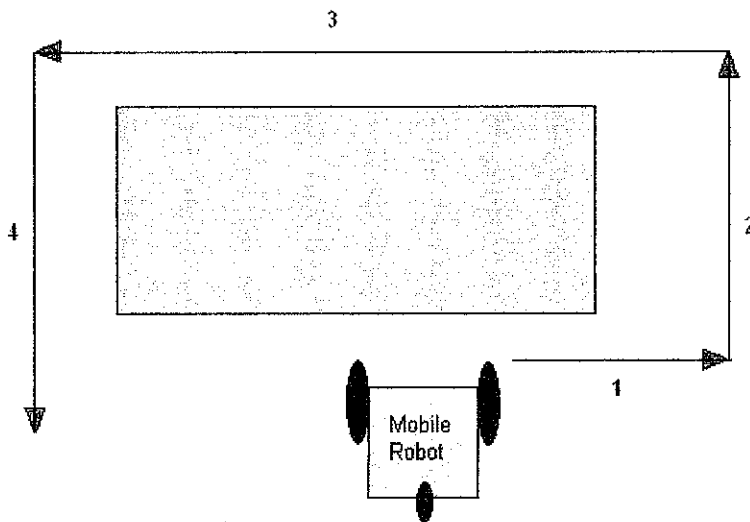


Figure 5.21 Predetermined paths for a mobile robot

Stage 1

When the robot senses an obstacle at its front, it will stop for 3.5 seconds. Subsequently, it will reverse for a very short period of time (approximately 0.16 seconds). Then, it turns right (with an angle of approximately 90°). It will pause for about 3.9 seconds before proceeding to the front for 2.1 seconds. After doing so, the robot will again pause for another 3.9 seconds.

Stage 2

The mobile robot reverses for a short while and turns left (approximately 90°). It then stops for 3.9 seconds. Subsequently, the robot continues on moving to the front for around 2.3 seconds. Finally, the robot stops for another 3.9 seconds before proceeding to stage 3.

Stage 3

At stage 3, the mobile robot again reverses for a short while before turning left. It then stops for 3.9 seconds and propels to the front for 3.4 seconds. After that, it stops for 3.9 seconds again.

Stage 4

In this last stage, the mobile robot reverses for a short period of time and then turns left. It stops for about 3.9 seconds again and move on to the front for 2.3 seconds. After doing so, the robot would take a long pause (14 seconds). This is to allow the user to choose either to reset the switch so as to switch back to obstacle avoidance mode or to continue executing the preprogrammed path.

The output waveforms from the microcontroller are observed using an oscilloscope and sketched. **Figure 5.21, 5.22, 5.23, 5.24** shows the pulses supplied to the H-bridge circuit to control the rotational direction of the 2 motors at stage 1, 2, 3, and 4 respectively.

Given that,

Left HB_1: The HB_1 pin in the H-bridge circuit shown in **Figure 3.1** that controls the left motor of the mobile robot.

Left HB_2: The HB_2 pin in the H-bridge circuit shown in **Figure 3.1** that controls the left motor of the mobile robot.

Right HB_1: The HB_1 pin in the H-bridge circuit shown in **Figure 3.1** that controls the right motor of the mobile robot.

Right HB_2: The HB_2 pin in the H-bridge circuit shown in **Figure 3.1** that controls the right motor of the mobile robot.

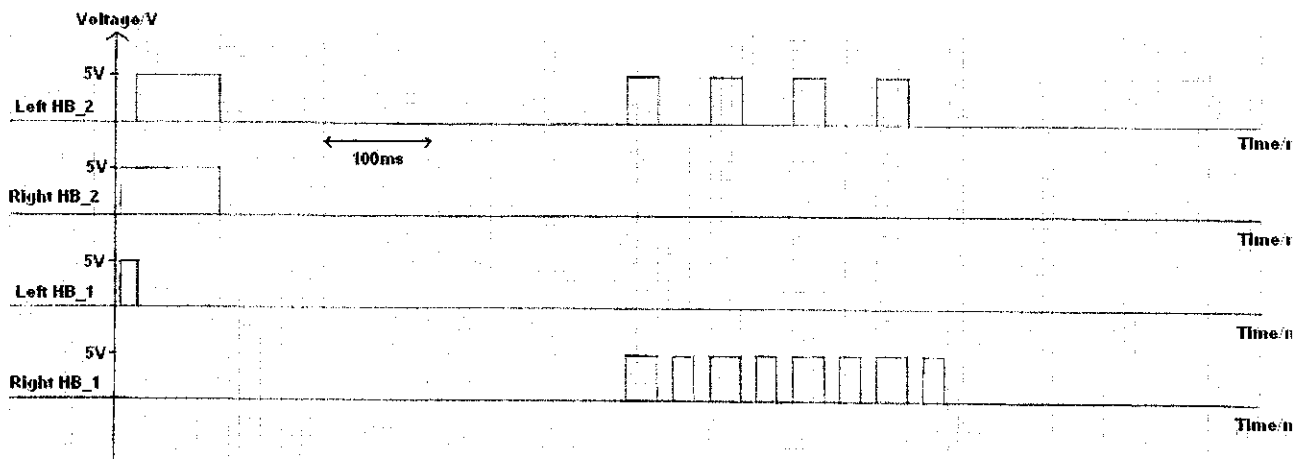


Figure 5.22 Pulses supplied to the H-bridge circuits in stage 1

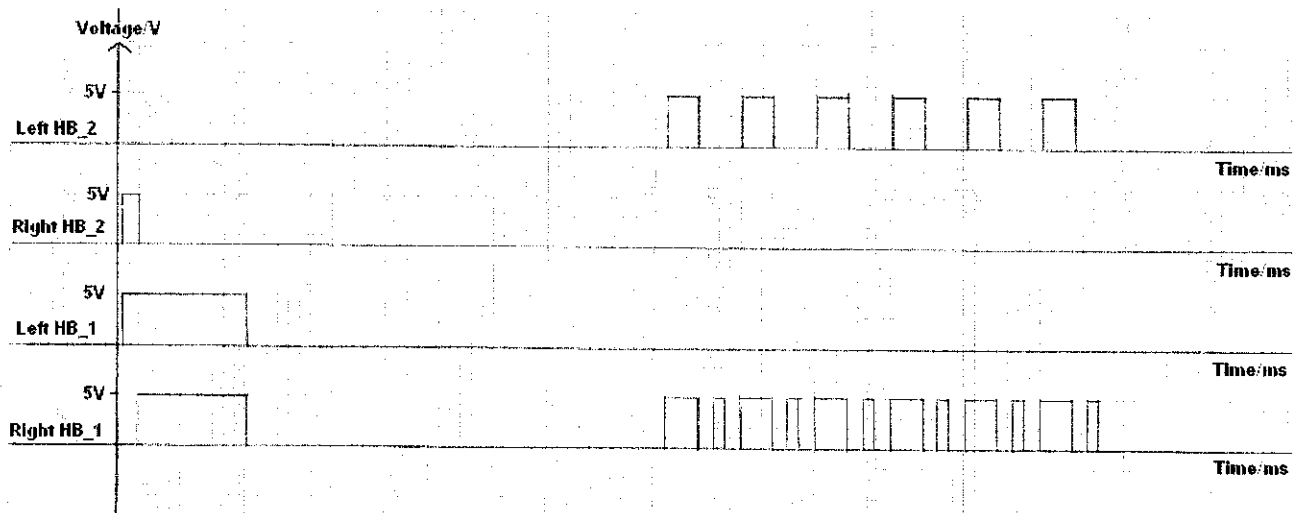


Figure 5.23 Pulses supplied to the H-bridge circuits in stage 2

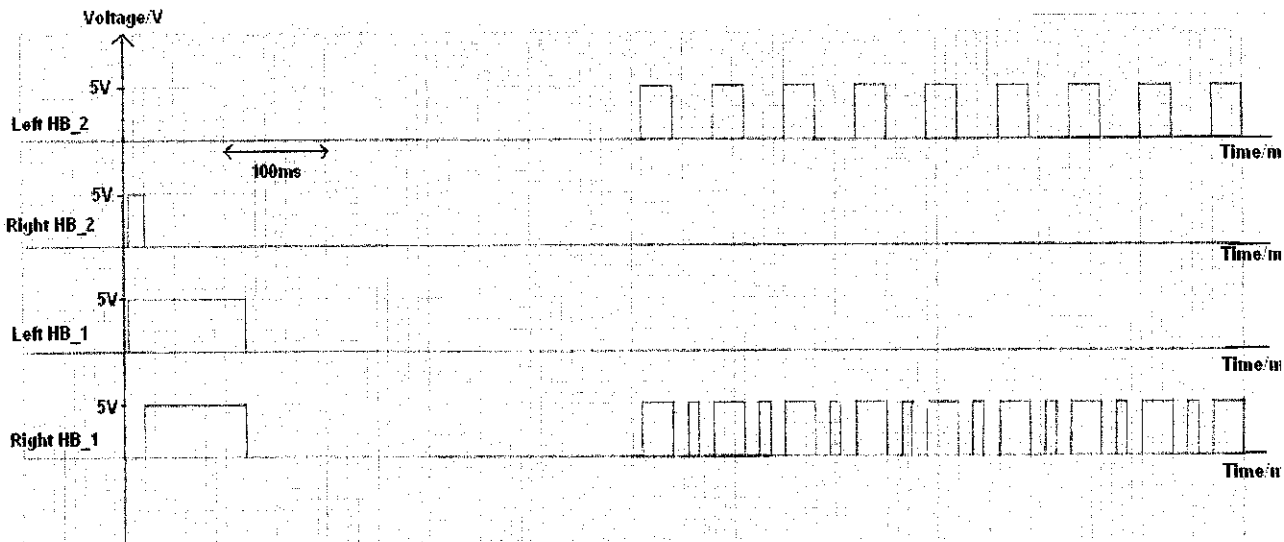


Figure 5.24 Pulses supplied to the H-bridge circuits in stage 3

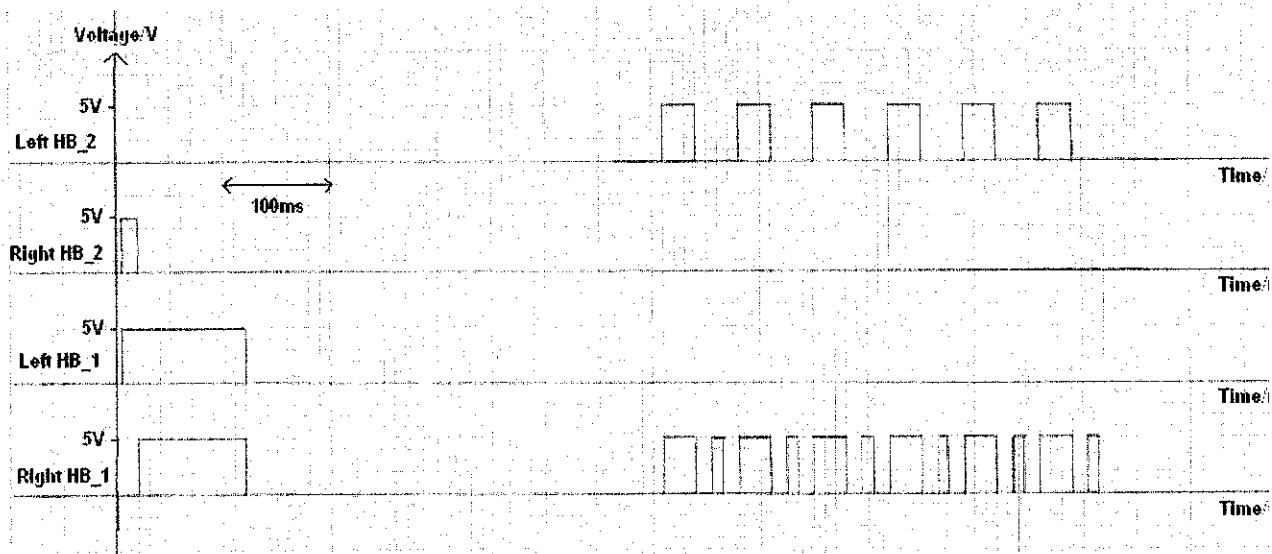


Figure 5.25 Pulses supplied to the H-bridge circuits in stage 4

5.5.3 Discussion

Problems Encountered and Methods of Corrections

One of the main problems encountered while building the mobile robot is the instability of the H-bridge circuit. It is noticed that the power MOSFETs (especially the P-channel MTP2955V MOSFET) tends to grow hot rather easily. If the heat is not dissipated appropriately, one may have to face the risk of damaging the H-bridge circuit and would, thus, end up failing to control the rotational direction of the dc motors. In order to cope with the problem, heat sink is suggested to be attached to the power MOSFETs. The heat sinks turn up to be rather effective and are capable of reducing the heat generated considerably. Another way of improvements is to allow the robot (the H-bridge circuits in particular) to pause and rest for every certain intervals. Time is given for the MOSFETs to cool down first before the next subsequent action is executed. In this case, the robot is programmed to take an approximate of 3.9s halt before proceeding to the next action.

Another problem that requires much attention is the weight of the battery. A 12V lead acid battery was used as the power supply for the mobile robot. The weight of the battery is around 1.5kg. The weight of the structure is around 3.5kg. Thus, if a lead acid battery is used, the load that the dc motors have to sustain is approximately 5kg. Much power was drawn in order to increase the torque of the motors. A solution to this problem, is to replace the lead acid battery with a 12V gel cell battery which weighs only about 0.57kg. This reduces the amount of current drawn to drive the robot.

Both the speeds of the 2 motors are different. Thus, the robot tends to divert to the right as the left motor turns faster than the right. A way to solve this problem is by giving different pulses to the H-bridge circuit. As can be seen in **Figure 5.22 to 5.25**, the pulses supplied to the right H-bridge is more than to the left. In this way, both the speed of the motors could be synchronized.

CHAPTER 6

CONCLUSION

The mobile robot consists of 3 main components – that is, ultrasonic sensors, h-bridge circuit, and a PIC16F84A microcontroller. The ultrasonic sensors serve the purpose of sensing obstacles ahead; whereas the h-bridge circuit controls the rotational direction of the motors. The microcontroller is considered as the most vital component among all. It is the brain of the robot and would be involved in decision-making.

This project serves the fundamental objective of allowing a student to gain some hand on experience on constructing a simple robot from scratch. By doing so, one would be able to apply the knowledge that one has learned thus far. This is especially true in the area of analogue electronics and microprocessor.

By studying on the operational theory of an H-bridge circuit, one would be able to gather a better understanding on BJT transistors and Power MOSFETs. Constructing an ultrasonic sensor allows a student to learn on the different applications of op-amp.

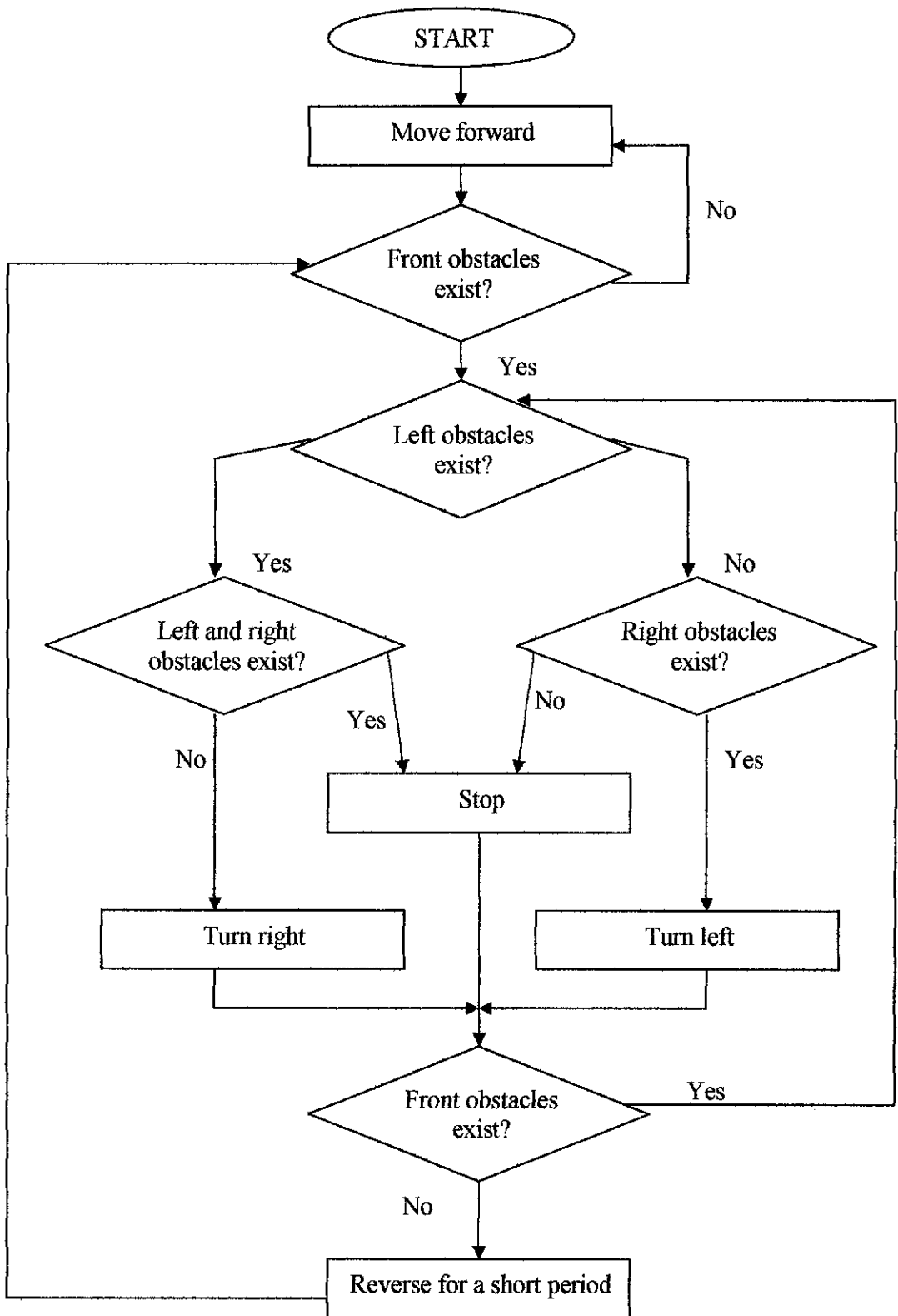
Simple as it may seem to be, an 8-bit microcontroller like PIC16F84A is in fact the perfect learning tool that allows a student to achieve a clear picture on the operation of a simple RISC architecture microprocessor. The student is also given the opportunity to get familiarized with writing programs using assembly code. Assembly code is a low level language that allows direct communication with the machine. A student could, thus, gain sufficient understanding on the very basic structure and function of a computer.

Finally, the mobile robot is a project that serves for research purposes. The functionalities that lie within are expected to be upgraded from time to time. This means that the intelligence of the robot would be enhanced by adding additional features to the robot. This may include putting fuzzy logic and neural network for route recognition, etc.

REFERENCES

1. Jaap Havinga, <<http://www.havingasoftware.nl/robots/snuf/snuf.htm>>
2. Francesco Mondada, June 1996 <<http://diwww.epfl.ch/lami/robots/K-family/K-family.html>>
3. Robot Room, <<http://www.robotroom.com/>>
4. Francesco Mondala, June, 1996 <<http://diwww.epfl.ch/lami/robots/K-family/Khepera.html>>
5. Pavel Baranov, 2002 <<http://www.picant.com/robot/robot.html>>
6. Gordon McComb, 2001, The Robot Builder's Bonanza, McGraw Hill
7. Karl Lunt, 2000, Build Your Own Robot, A K Peters Natick, Massachusetts
8. Koji Soshino, 1999 <http://www2.plala.or.jp/k_y_yoshino/eng/index.html>

APPENDIX A
ALGORITHM FOR OBSTACLES AVOIDANCE



APPENDIX B

SOURCE CODE FOR OBSTACLES AVOIDANCE AND PATH FINDING

Title: "DESIGN AND IMPLEMENTATION OF A MOBILE ROBOT"

List p=16f84

;Processor type

;-----

;- INITIALIZATION -

;-----

```
PORT_A    equ    0X05
PORT_B    equ    0X06
TEMP1     equ    0x0C           ;Temp variables
TEMP2     equ    0x0D
TEMP3     equ    0x0E
COUNTER   equ    0x0F
BIGLOOP   equ    0x10
SENSOR_L  equ    1
SENSOR_R  equ    2
SENSOR_F  equ    3
SW_L      equ    4
SW_R      equ    5
PATHFIND  equ    6
HB_1_L    equ    0
HB_2_L    equ    1
HB_1_R    equ    2
HB_2_R    equ    3
```

;-----

;- MAIN -

;-----

```
org    0H
movlw  b'00000000'
tris   PORT_A
clrf   PORT_A
movlw  b'11111111'
tris   PORT_B
clrf   PORT_B
```

```

        clrf    TEMP1
        clrf    TEMP2
        clrf    TEMP3
        clrf    COUNTER
        bsf     PORT_B,7

FRONT    call    START
        btfsz   PORT_B,SENSOR_F    ;Check front obstacle
        goto    LEFT_RIGHT         ;If front obstacle exists, check if left-right
                                        ;obstacle exists
        goto    FRONT              ;If not, keep checking if front obstacle exists

LEFT_RIGHT btfsz   PORT_B,SENSOR_L    ;Check left obstacle
        goto    LEFT_1_RIGHT         ;If left obstacle exists, check right obstacle
        goto    LEFT_0_RIGHT        ;If left obstacle doesn't exist, check right
                                        ;obstacle

LEFT_1_RIGHT btfsz   PORT_B,SENSOR_R    ;If left obstacle exists, check right obstacle
        goto    STOP                ;If front, left, right obstacle exists, robot stop
                                        ;moving
        goto    RIGHT              ;If front, left obstacle exists, robot turn right

LEFT_0_RIGHT btfsz   PORT_B,SENSOR_R    ;If left obstacle doesn't exist, check right
                                        ;obstacle
        goto    LEFT                ;If front, right obstacle exists, robot turn left
        goto    DEFAULT            ;if only front obstacle exists, robot stops or take
                                        ;the default route

STOP     bcf     PORT_A,HB_1_L        ;0 output to left h-bridge1
        bcf     PORT_A,HB_2_R        ;0 output to right h-bridge2
        bcf     PORT_A,HB_1_R        ;0 output to right h-bridge1
        bcf     PORT_A,HB_2_L        ;0 output to left h-bridge2
        clrf    COUNTER
        movlw   0x04
        movwf   COUNTER

DURATION1 call    DELAY              ;robot stops for 1.6sec
        decfsz  COUNTER
        goto    DURATION1
        goto    FRONT

```

```

RIGHT      call    REVERSE          ;robot reverses for 0.8sec
           clrf    COUNTER
           movlw  0x02
           movwf  COUNTER
DURATION2  call    DELAY
           decfsz COUNTER
           goto   DURATION2
           bcf    PORT_A,HB_1_L      ;0 output to left h-bridge1
           bcf    PORT_A,HB_2_L      ;0 output to left h-bridge2
           bsf    PORT_A,HB_1_R      ;1 output to right h-bridge1
           bsf    PORT_A,HB_2_R      ;1 output to right h-bridge2
           clrf    COUNTER
           movlw  0x01
           movwf  COUNTER
DURATION3  call    DELAY          ;robot then turn right for 0.9sec
           decfsz COUNTER
           goto   DURATION3
           call   DELAY
           call   DELAY2
           call   PAUSE             ;robot halts for 3.5sec
           goto   FRONT
           .
LEFT       call    REVERSE          ;robot reverses for 0.8sec
           clrf    COUNTER
           movlw  0x02
           movwf  COUNTER
DURATION4  call    DELAY
           decfsz COUNTER
           goto   DURATION4
           bcf    PORT_A,HB_1_R      ;0 output to right h-bridge1
           bcf    PORT_A,HB_2_R      ;0 output to right h-bridge2
           bsf    PORT_A,HB_1_L      ;1 output to left h-bridge1
           bsf    PORT_A,HB_2_L      ;1 output to left h-bridge2
           clrf    COUNTER
           movlw  0x01
           movwf  COUNTER
DURATION5  call    DELAY          ;robot then turn left for 0.9sec
           .
           decfsz COUNTER
           goto   DURATION5

```

```

call    DELAY
call    DELAY2
call    PAUSE           ;robot halts for 3.5sec
goto    FRONT

DEFAULT  btfss  PORT_B,PATHFIND  ;check if PATHFIND switch is on
goto    PATH_RIGHT1    ;if yes, robot manoeuvre on predetermined path
bcf     PORT_A,HB_1_L  ;0 output to left h-bridge1
bcf     PORT_A,HB_2_R  ;0 output to right h-bridge2
bcf     PORT_A,HB_1_R  ;0 output to right h-bridge1
bcf     PORT_A,HB_2_L  ;0 output to left h-bridge2
clrf    COUNTER
movlw  0x0A
movwf  COUNTER

DURATION6 call  DELAY           ;if no, robot stops for 3.9sec
decsz  COUNTER
goto   DURATION6
goto   FRONT

;-----
;- SUBROUTINE -
;-----

START  btfsc  PORT_B,SENSOR_F  ;check if front obstacle exists
goto   LEFT_RIGHT            ;if yes, check if left and right obstacles exists
bcf    PORT_A,HB_1_L          ;0 output to left h-bridge1
bcf    PORT_A,HB_2_R          ;0 output to right h-bridge2
bsf    PORT_A,HB_1_R          ;1 output to right h-bridge1
bsf    PORT_A,HB_2_L          ;1 output to left h-bridge2
call   DELAY2                 ;if only front obstacle exists, go straight for
                                ;0.16sec
call   ZERO                   ;robot halts for 0.15sec
call   DELAY3                 ;to balance both the speed of the motor,
bcf    PORT_A,HB_1_L          ;0 output to left h-bridge1
bcf    PORT_A,HB_2_R          ;0 output to left h-bridge2
bsf    PORT_A,HB_1_R          ;0 output to right h-bridge1
bcf    PORT_A,HB_2_L          ;1 output to right h-bridge2
call   DELAY4                 ;left motor turns, while right motor rests for
                                ;0.04sec
call   ZERO                   ;robot halts for 0.15sec

```

```

call    DELAY3
return

```

```

REVERSE    bcf    PORT_A,HB_2_L    ;0 output to left h-bridge2
           bcf    PORT_A,HB_1_R    ;0 output to right h-bridge1
           bsf    PORT_A,HB_2_R    ;1 output to right h-bridge2
           bsf    PORT_A,HB_1_L    ;1 output to left h-bridge1
           return                    ;robot reverses

```

```

;-----
;- PATH FINDING -
;-----

```

```

;           3
;
;           _____
;           |         |
;           4|         |
;           |         | 2
;           |         |
;           |         |
;           |         | 1
;           |         |
;           |         |
;           |         |

```

```
;- 1 -
```

```

PATH_RIGHT1 call    PAUSE            ;robot halts for 3.5sec
           call    REVERSE          ;robot reverses for 0.16sec
           clrf   COUNTER
           movlw  0x01
           movwf  COUNTER
P_DURATION1 call    DELAY2
           decfsz COUNTER
           goto   P_DURATION1
           call   TURNRIGHT          ;robot turns right for 0.82sec
           clrf   COUNTER
           movlw  0x02
           movwf  COUNTER
P_DURATION2 call    DELAY
           decfsz COUNTER
           goto   P_DURATION2

```

```

                call    DELAY4

;- 1 -
PATH_STOP1    call    PAUSE                ;robot halts for 3.9sec
                call    DELAY

;- 1 -
PATH_FORWARD1    clrf    COUNTER        ;robot propel forward for 2.1sec
                movlw  0x04
                movwf  COUNTER
P_DURATION3    call    STRAIGHT3
                decfsz COUNTER
                goto   P_DURATION3
                call    DELAY3

;- 1 -
PATH_STOP2    call    PAUSE                ;robot halts for 3.9sec
                call    DELAY

;- 2 -
PATH_LEFT1    call    REVERSE            ;robot reverses for 0.16sec
                clrf    COUNTER
                movlw  0x01
                movwf  COUNTER
P_DURATION4    call    DELAY2
                decfsz COUNTER
                goto   P_DURATION4
                call    TURNLEFT        ;robot turns left for 1.0sec
                clrf    COUNTER
                movlw  0x02
                movwf  COUNTER
P_DURATION5    call    DELAY
                decfsz COUNTER
                goto   P_DURATION5
                call    DELAY4
                call    DELAY4
                call    DELAY2

```

;- 2 -

```
PATH_STOP3 call PAUSE           ;robot halts for 3.9sec
           call DELAY
```

;- 2 -

```
PATH_FORWARD2 clrf COUNTER      ;robot propels forward for 2.3sec
              movlw 0x06
              movwf COUNTER
P_DURATION6 call STRAIGHT
              decfsz COUNTER
              goto P_DURATION6
              call DELAY3
```

;- 2 -

```
PATH_STOP4 call PAUSE           ;robot halts for 3.9sec
           call DELAY
```

;- 3 -

```
PATH_LEFT2 call REVERSE         ;robot reverses for 0.16sec
           clrf COUNTER
           movlw 0x01
           movwf COUNTER
P_DURATION7 call DELAY2
           decfsz COUNTER
           goto P_DURATION7
           call TURNLEFT        ;robot turns left for 0.97sec
           clrf COUNTER
           movlw 0x02
           movwf COUNTER
P_DURATION8 call DELAY
           decfsz COUNTER
           goto P_DURATION8
           call DELAY4
           call DELAY3
```

;- 3 -

```
PATH_STOP5 call PAUSE           ;robot halts for 3.9sec
           call DELAY
```

;- 3 -

```
PATH_FORWARD3    clrf    COUNTER    ;robot propels forward for 3.4sec
                 movlw  0x09
                 movwf  COUNTER
P_DURATION9      call    STRAIGHT
                 decfsz COUNTER
                 goto   P_DURATION9
                 call   DELAY3
```

;- 3 -

```
PATH_STOP6       call    PAUSE        ;robot halts for 3.9sec
                 call   DELAY
```

;- 4 -

```
PATH_LEFT3       call    REVERSE      ;robot reverses for 0.16sec
                 clrf    COUNTER
                 movlw  0x01
                 movwf  COUNTER
P_DURATION10     call    DELAY2
                 decfsz COUNTER
                 goto   P_DURATION10
                 call   TURNLEFT      ;robot turns left for 0.97sec
                 clrf    COUNTER
                 movlw  0x02
                 movwf  COUNTER
P_DURATION11     call    DELAY
                 decfsz COUNTER
                 goto   P_DURATION11
                 call   DELAY4
                 call   DELAY3
```

;- 4 -

```
PATH_STOP7       call    PAUSE        ;robot halts for 3.9sec
                 call   DELAY
```

;- 4 -

```
PATH_FORWARD4    clrf    COUNTER    ;robot propels forward for 2.3sec
                 movlw  0x06
                 movwf  COUNTER
```

```

P_DURATION12    call    STRAIGHT
                decfsz  COUNTER
                goto    P_DURATION12
                call    DELAY3

;- FINAL -
PATH_STOPF     call    PAUSE                ;robot halts for 14sec
                clrf    COUNTER
                movlw   0x1A
                movwf   COUNTER
P_DURATIONF    call    DELAY
                decfsz  COUNTER
                goto    P_DURATIONF
                goto    FRONT

;-----
;- PATH SUBROUTINE -
;-----

DELAY          movlw   0xFF                ;a delay of approximately 0.39s
                movwf   TEMP1
DLOOP1         movlw   0xFF
                movwf   TEMP2
                movwf   TEMP3
DLOOP2         decfsz  TEMP2
                goto    DLOOP2
DLOOP3         decfsz  TEMP3
                goto    DLOOP3
                decfsz  TEMP1
                goto    DLOOP1
                return

DELAY2         movlw   0xD0                ;a delay of approximately 0.16s
                movwf   TEMP1
DLOOP4         movlw   0xFF
                movwf   TEMP2
DLOOP5         decfsz  TEMP2
                goto    DLOOP5
                decfsz  TEMP1

```

```

goto    DLOOP4
return

DELAY3   movlw  0xC0           ;a delay of approximately 0.15s
         movwf  TEMP1

DLOOP6   movlw  0xFF
         movwf  TEMP2

DLOOP7   decfsz TEMP2
         goto   DLOOP7
         decfsz TEMP1
         goto   DLOOP6
         return

DELAY4   movlw  0x55           ;a delay of approximately 0.04s
         movwf  TEMP1

DLOOP8   movlw  0xA0
         movwf  TEMP2

DLOOP9   decfsz TEMP2
         goto   DLOOP9
         decfsz TEMP1
         goto   DLOOP8
         return

STRAIGHT bcf    PORT_A,HB_1_L   ;0 output to left h-bridge1
         bcf    PORT_A,HB_2_R   ;0 output to right h-bridge2
         bsf    PORT_A,HB_1_R   ;1 output to right h-bridge1
         bsf    PORT_A,HB_2_L   ;1 output to left h-bridge2
         call   DELAY3          ;go straight for 0.30s
         call   DELAY3
         call   ZERO           ;halt for 0.15s
         call   DELAY3
         bcf    PORT_A,HB_1_L   ;0 output to left h-bridge1
         bcf    PORT_A,HB_2_R   ;0 output to left h-bridge2
         bsf    PORT_A,HB_1_R   ;0 output to right h-bridge1
         bcf    PORT_A,HB_2_L   ;1 output to right h-bridge2
         call   DELAY4          ;left motor runs while right motor stops for 0.08s
         call   DELAY4          ;to balance the speed of both motor
         call   ZERO           ;halt for 0.15s
         call   DELAY3
         return

```

```

STRAIGHT2  bcf    PORT_A,HB_1_L    ;0 output to left h-bridge1
            bcf    PORT_A,HB_2_R    ;0 output to right h-bridge2
            bsf    PORT_A,HB_1_R    ;1 output to right h-bridge1
            bsf    PORT_A,HB_2_L    ;1 output to left h-bridge2
            call   DELAY2            ;go straight for0.16s
            call   ZERO              ;halt for 0.04s
            call   DELAY4
            return

STRAIGHT3  bcf    PORT_A,HB_1_L    ;0 output to left h-bridge1
            bcf    PORT_A,HB_2_R    ;0 output to right h-bridge2
            bsf    PORT_A,HB_1_R    ;1 output to right h-bridge1
            bsf    PORT_A,HB_2_L    ;1 output to left h-bridge2
            call   DELAY3            ;go straight for 0.30s
            call   DELAY3
            call   ZERO              ;halt for 0.15s
            call   DELAY3
            bcf    PORT_A,HB_1_L    ;0 output to left h-bridge1
            bcf    PORT_A,HB_2_R    ;0 output to left h-bridge2
            bsf    PORT_A,HB_1_R    ;0 output to right h-bridge1
            bcf    PORT_A,HB_2_L    ;1 output to right h-bridge2
            call   DELAY3            ;left motor runs while right motor stops for 0.19s
            call   DELAY4            ;to balance the speed of the motor
            call   ZERO              ;halt for 0.15s
            call   DELAY3
            return

TURNRIGHT  bcf    PORT_A,HB_1_R    ;0 output to right h-bridge1
            bcf    PORT_A,HB_2_R    ;0 output to right h-bridge2
            bsf    PORT_A,HB_1_L    ;1 output to left h-bridge1
            bsf    PORT_A,HB_2_L    ;1 output to left h-bridge2
            return

TURNLEFT   bcf    PORT_A,HB_1_L    ;0 output to left h-bridge1
            bcf    PORT_A,HB_2_L    ;0 output to left h-bridge2
            bsf    PORT_A,HB_1_R    ;1 output to right h-bridge1
            bsf    PORT_A,HB_2_R    ;1 output to right h-bridge2
            return

ZERO       bcf    PORT_A,HB_1_R    ;0 output to left h-bridge1

```

```

        bcf    PORT_A,HB_2_R    ;0 output to left h-bridge2
        bcf    PORT_A,HB_1_L    ;0 output to right h-bridge1
        bcf    PORT_A,HB_2_L    ;0 output to right h-bridge2
        return

PAUSE   bcf    PORT_A,HB_1_R    ;0 output to left h-bridge1
        bcf    PORT_A,HB_2_R    ;0 output to left h-bridge2
        bcf    PORT_A,HB_1_L    ;0 output to right h-bridge1
        bcf    PORT_A,HB_2_L    ;0 output to right h-bridge2
        clrf   COUNTER          ;halt for 3.5s
        movlw 0x09
        movwf  COUNTER

PAUSE_DELAY call  DELAY
        decfsz COUNTER
        goto  PAUSE_DELAY
        return

        end

```

APPENDIX C

MTP2955V P-CHANNEL MOSFET DATASHEET

MTP2955V

Preferred Device

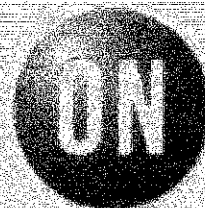
Power MOSFET 12 Amps, 60 Volts P-Channel TO-220

This Power MOSFET is designed to withstand high energy in the avalanche and commutation modes. Designed for low voltage, high speed switching applications in power supplies, converters and power motor controls, these devices are particularly well suited for bridge circuits where diode speed and commutating safe operating areas are critical and offer additional safety margin against unexpected voltage transients.

- Avalanche Energy Specified
- I_{DSS} and $V_{DS(on)}$ Specified at Elevated Temperature

MAXIMUM RATINGS ($T_C = 25^\circ\text{C}$ unless otherwise noted)

Rating	Symbol	Value	Unit
Drain-to-Source Voltage	V_{DS}	60	Vdc
Drain-to-Gate Voltage ($R_{GS} = 1.0\text{ M}\Omega$)	V_{DGR}	60	Vdc
Gate-to-Source Voltage	V_{GS}	± 15	Vdc
- Continuous	V_{GS}	± 15	Vdc
- Non-Repetitive ($t_p \leq 10\text{ ms}$)	V_{GSM}	± 25	Vpk
Drain Current - Continuous	I_D	12	Adc
- Continuous @ 100°C	I_D	8.0	Adc
- Single Pulse ($t_p \leq 10\text{ }\mu\text{s}$)	I_{DM}	42	Apk
Total Power Dissipation Derate above 25°C	P_D	60 0.40	Watts W/ $^\circ\text{C}$
Operating and Storage Temperature Range	T_J, T_{stg}	-55 to 175	$^\circ\text{C}$
Single Pulse Drain-to-Source Avalanche Energy - Starting $T_J = 25^\circ\text{C}$ ($V_{DD} = 25\text{ Vdc}$, $V_{GS} = 10\text{ Vdc}$, Peak $I_L = 12\text{ Apk}$, $L = 3.0\text{ mH}$, $R_G = 25\text{ }\Omega$)	EAS	216	mJ
Thermal Resistance	$R_{\theta JC}$ $R_{\theta JA}$	2.5 62.5	$^\circ\text{C/W}$
Maximum Lead Temperature for Soldering Purposes, $1/8"$ from case for 10 seconds	T_L	260	$^\circ\text{C}$



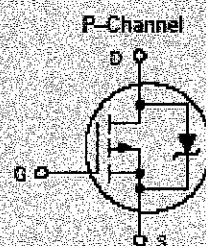
ON Semiconductor™

<http://onsemi.com>

12 AMPERES

60 VOLTS

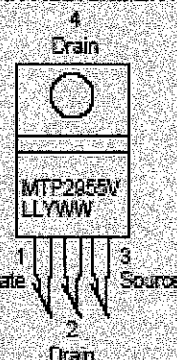
$R_{DS(on)} = 230\text{ m}\Omega$



MARKING DIAGRAM & PIN ASSIGNMENT



TO-220AB
CASE 221A
STYLE 5



MTP2955V = Device Code
LL = Location Code
Y = Year
WW = Work Week

ORDERING INFORMATION

Device	Package	Shipping
MTP2955V	TO-220AB	50 Units/Rol

Preferred devices are recommended choices for future use and best overall value.

MTP2955V

ELECTRICAL CHARACTERISTICS ($T_J = 25^\circ\text{C}$ unless otherwise noted)

Characteristic	Symbol	Min	Typ	Max	Unit	
OFF CHARACTERISTICS						
Drain-to-Source Breakdown Voltage ($V_{GS} = 0\text{ Vdc}$, $I_D = 0.25\text{ mAdc}$) Temperature Coefficient (Positive)	$V_{(BR)DSS}$	60 -	- 58	- -	Vdc mV/°C	
Zero Gate Voltage Drain Current ($V_{DS} = 60\text{ Vdc}$, $V_{GS} = 0\text{ Vdc}$) ($V_{DS} = 60\text{ Vdc}$, $V_{GS} = 0\text{ Vdc}$, $T_J = 150^\circ\text{C}$)	I_{DSS}	- -	- -	10 100	μA	
Gate-Body Leakage Current ($V_{GS} = \pm 15\text{ Vdc}$, $V_{DS} = 0\text{ Vdc}$)	I_{GSS}	-	-	100	nA	
ON CHARACTERISTICS (Note 1.)						
Gate Threshold Voltage ($V_{DS} = V_{GS}$, $I_D = 250\ \mu\text{A}$) Threshold Temperature Coefficient (Negative)	$V_{GS(th)}$	2.0 -	2.8 5.0	4.0 -	Vdc mV/°C	
Static Drain-to-Source On-Resistance ($V_{GS} = 10\text{ Vdc}$, $I_D = 6.0\text{ Adc}$)	$R_{DS(on)}$	-	0.185	0.230	Ohm	
Drain-to-Source On-Voltage ($V_{GS} = 10\text{ Vdc}$, $I_D = 12\text{ Adc}$) ($V_{GS} = 10\text{ Vdc}$, $I_D = 6.0\text{ Adc}$, $T_J = 150^\circ\text{C}$)	$V_{DS(on)}$	- -	- -	2.9 2.5	Vdc	
Forward Transconductance ($V_{DS} = 10\text{ Vdc}$, $I_D = 6.0\text{ Adc}$)	g_{FS}	3.0	6.0	-	mhos	
DYNAMIC CHARACTERISTICS						
Input Capacitance	$(V_{DS} = 25\text{ Vdc}$, $V_{GS} = 0\text{ Vdc}$, $f = 1.0\text{ MHz}$)	C_{iss}	-	550	700	μF
Output Capacitance		C_{oss}	-	200	280	
Reverse Transfer Capacitance		C_{rss}	-	50	100	
SWITCHING CHARACTERISTICS (Note 2.)						
Turn-On Delay Time	$(V_{DD} = 30\text{ Vdc}$, $I_D = 12\text{ Adc}$, $V_{GS} = 10\text{ Vdc}$, $R_G = 9.1\ \Omega$)	$t_{d(on)}$	-	15	30	ns
Rise Time		t_r	-	50	100	
Turn-Off Delay Time		$t_{d(off)}$	-	24	50	
Fall Time		t_f	-	39	80	
Gate Charge	$(V_{DS} = 48\text{ Vdc}$, $I_D = 12\text{ Adc}$, $V_{GS} = 10\text{ Vdc}$)	Q_T	-	19	30	nC
		Q_1	-	4.0	-	
		Q_2	-	9.0	-	
		Q_3	-	7.0	-	
SOURCE-DRAIN DIODE CHARACTERISTICS						
Forward On-Voltage (Note 1.)	$(I_S = 12\text{ Adc}$, $V_{GS} = 0\text{ Vdc}$) $(I_S = 12\text{ Adc}$, $V_{GS} = 0\text{ Vdc}$, $T_J = 150^\circ\text{C}$)	V_{SD}	- -	1.8 1.5	3.0 -	Vdc
Reverse Recovery Time		$(I_S = 12\text{ Adc}$, $V_{GS} = 0\text{ Vdc}$, $di_S/dt = 100\text{ A}/\mu\text{s}$)	t_{rr}	-	115	-
	t_a		-	90	-	
	t_b		-	25	-	
Reverse Recovery Stored Charge	Q_{RR}		-	0.53	-	μC
INTERNAL PACKAGE INDUCTANCE						
Internal Drain Inductance (Measured from the drain lead 0.25" from package to center of die)	L_D	-	4.5	-	nH	
Internal Source Inductance (Measured from the source lead 0.25" from package to source bond pad)	L_S	-	7.5	-	nH	

1. Pulse Test: Pulse Width $\leq 300\ \mu\text{s}$, Duty Cycle $\leq 2\%$.
2. Switching characteristics are independent of operating junction temperature.
3. Reflects typical values. $C_{pk} = \left| \frac{\text{Max (min) - Typ}}{3 \times \text{SIGMA}} \right|$

MTP2955V

TYPICAL ELECTRICAL CHARACTERISTICS

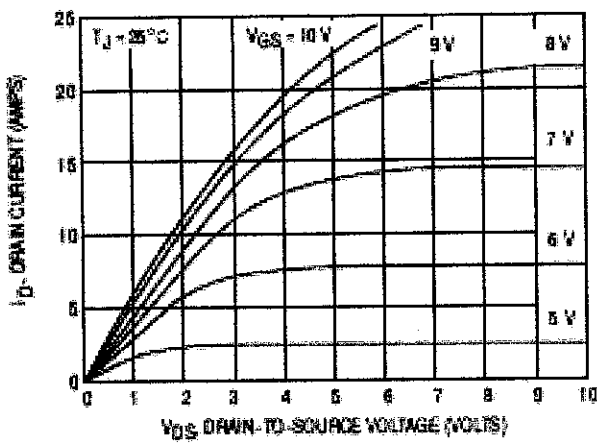


Figure 1. On-Region Characteristics

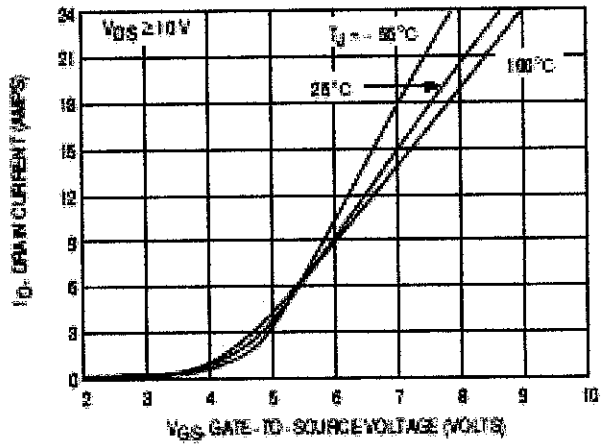


Figure 2. Transfer Characteristics

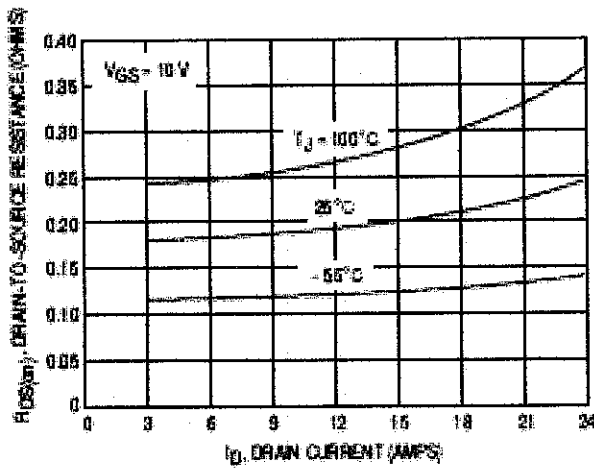


Figure 3. On-Resistance versus Drain Current and Temperature

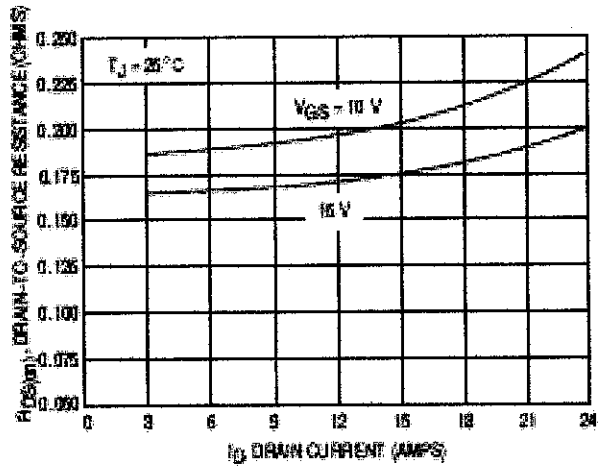


Figure 4. On-Resistance versus Drain Current and Gate Voltage

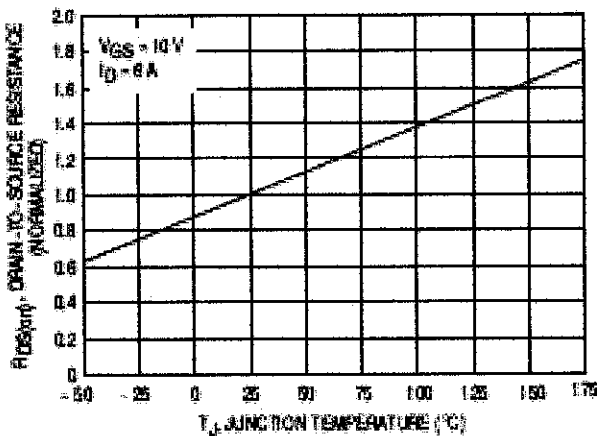


Figure 5. On-Resistance Variation with Temperature

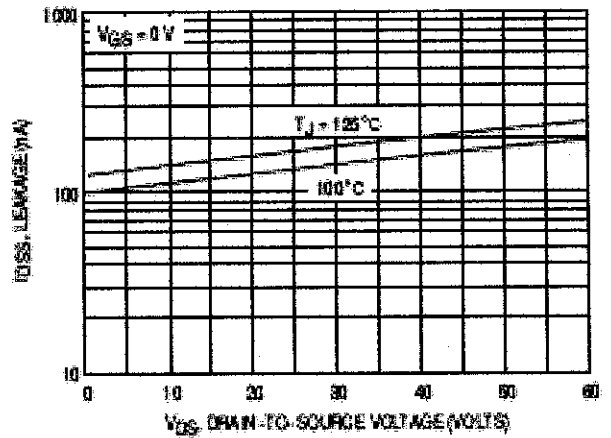


Figure 6. Drain-To-Source Leakage Current versus Voltage

MTP2955V

POWER MOSFET SWITCHING

Switching behavior is most easily modeled and predicted by recognizing that the power MOSFET is charge controlled. The lengths of various switching intervals (Δt) are determined by how fast the FET input capacitance can be charged by current from the generator. The published capacitance data is difficult to use for calculating rise and fall because drain-gate capacitance varies greatly with applied voltage. Accordingly, gate charge data is used. In most cases, a satisfactory estimate of average input current ($I_{G(AV)}$) can be made from a rudimentary analysis of the drive circuit so that

$$t = Q/I_{G(AV)}$$

During the rise and fall time interval when switching a resistive load, V_{GS} remains virtually constant at a level known as the plateau voltage, V_{GSP} . Therefore, rise and fall times may be approximated by the following:

$$t_r = Q_2 \times R_G / (V_{GG} - V_{GSP})$$

$$t_f = Q_2 \times R_G / V_{GSP}$$

where

V_{GG} = the gate drive voltage, which varies from zero to V_{GG}

R_G = the gate drive resistance

and Q_2 and V_{GSP} are read from the gate charge curve.

During the turn-on and turn-off delay times, gate current is not constant. The simplest calculation uses appropriate values from the capacitance curves in a standard equation for voltage change in an RC network. The equations are:

$$t_{d(on)} = R_G C_{iss} \ln [V_{GG}/(V_{GG} - V_{GSP})]$$

$$t_{d(off)} = R_G C_{iss} \ln (V_{GG}/V_{GSP})$$

The capacitance (C_{iss}) is read from the capacitance curve at a voltage corresponding to the off-state condition when calculating $t_{d(on)}$ and is read at a voltage corresponding to the on-state when calculating $t_{d(off)}$.

At high switching speeds, parasitic circuit elements complicate the analysis. The inductance of the MOSFET source lead, inside the package and in the circuit wiring which is common to both the drain and gate current paths, produces a voltage at the source which reduces the gate drive current. The voltage is determined by $L di/dt$, but since di/dt is a function of drain current, the mathematical solution is complex. The MOSFET output capacitance also complicates the mathematics. And finally, MOSFETs have finite internal gate resistance which effectively adds to the resistance of the driving source, but the internal resistance is difficult to measure and, consequently, is not specified.

The resistive switching time variation versus gate resistance (Figure 9) shows how typical switching performance is affected by the parasitic circuit elements. If the parasitics were not present, the slope of the curves would maintain a value of unity regardless of the switching speed. The circuit used to obtain the data is constructed to minimize common inductance in the drain and gate circuit loops and is believed readily achievable with board mounted components. Most power electronic loads are inductive; the data in the figure is taken with a resistive load, which approximates an optimally snubbed inductive load. Power MOSFETs may be safely operated into an inductive load; however, snubbing reduces switching losses.

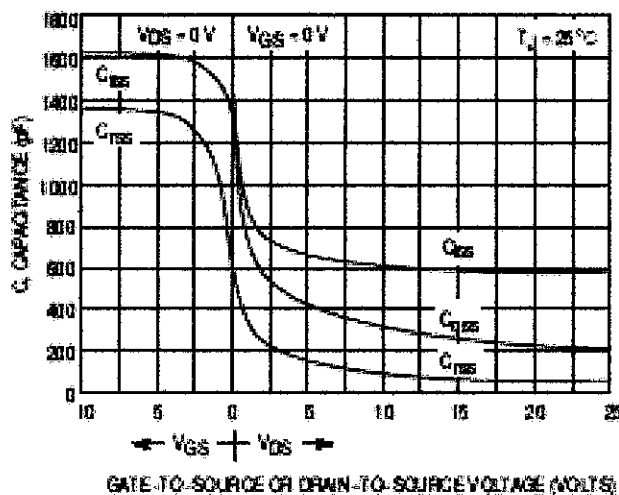


Figure 7. Capacitance Variation

MTP2955V

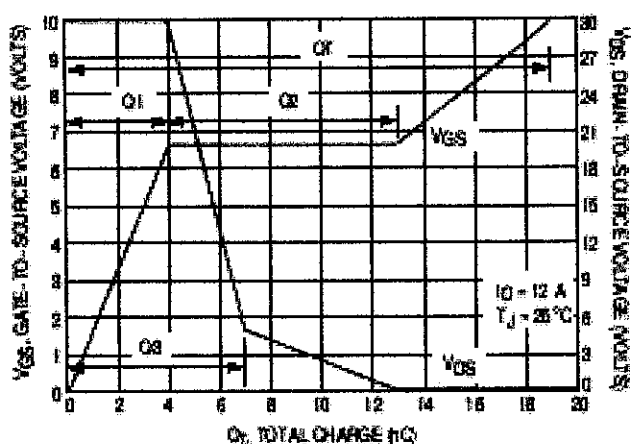


Figure 8. Gate-To-Source and Drain-To-Source Voltage versus Total Charge

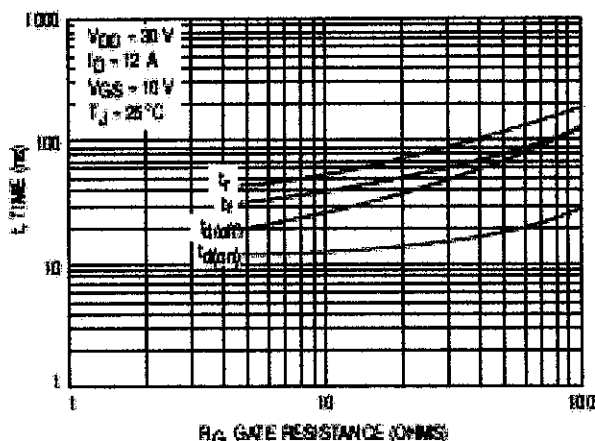


Figure 9. Relative Switching Time Variation versus Gate Resistance

DRAIN-TO-SOURCE DIODE CHARACTERISTICS

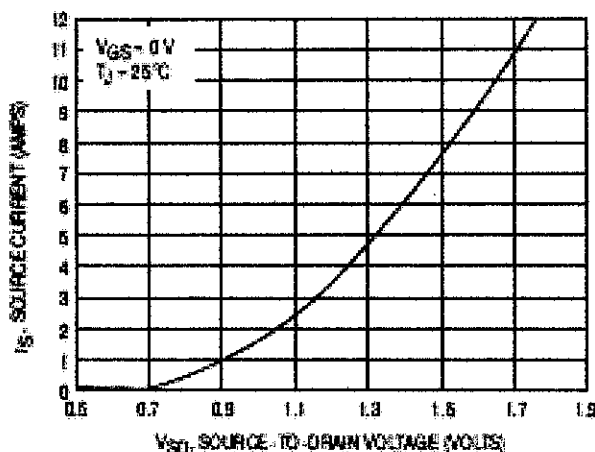


Figure 10. Diode Forward Voltage versus Current

SAFE OPERATING AREA

The Forward Biased Safe Operating Area curves define the maximum simultaneous drain-to-source voltage and drain current that a transistor can handle safely when it is forward biased. Curves are based upon maximum peak junction temperature and a case temperature (T_C) of 25°C. Peak repetitive pulsed power limits are determined by using the thermal response data in conjunction with the procedures discussed in AN569, "Transient Thermal Resistance—General Data and Its Use."

Switching between the off-state and the on-state may traverse any load line provided neither rated peak current (I_{DM}) nor rated voltage (V_{DSS}) is exceeded and the transition time (t_r, t_f) do not exceed 10 μ s. In addition the total power averaged over a complete switching cycle must not exceed $(T_J(\text{MAX}) - T_C)/(R_{\theta JC})$.

A Power MOSFET designated E-FET can be safely used in switching circuits with unclamped inductive loads. For

reliable operation, the stored energy from circuit inductance dissipated in the transistor while in avalanche must be less than the rated limit and adjusted for operating conditions differing from those specified. Although industry practice is to rate in terms of energy, avalanche energy capability is not a constant. The energy rating decreases non-linearly with an increase of peak current in avalanche and peak junction temperature.

Although many E-FETs can withstand the stress of drain-to-source avalanche at currents up to rated pulsed current (I_{DM}), the energy rating is specified at rated continuous current (I_D), in accordance with industry custom. The energy rating must be derated for temperature as shown in the accompanying graph (Figure 13). Maximum energy at currents below rated continuous I_D can safely be assumed to equal the values indicated.

MTP2955V

SAFE OPERATING AREA

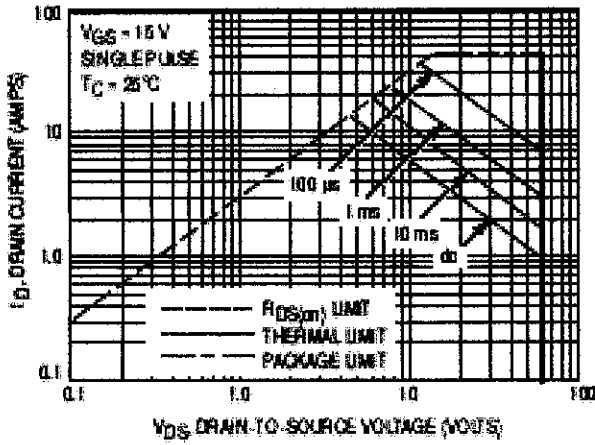


Figure 11. Maximum Rated Forward Biased Safe Operating Area

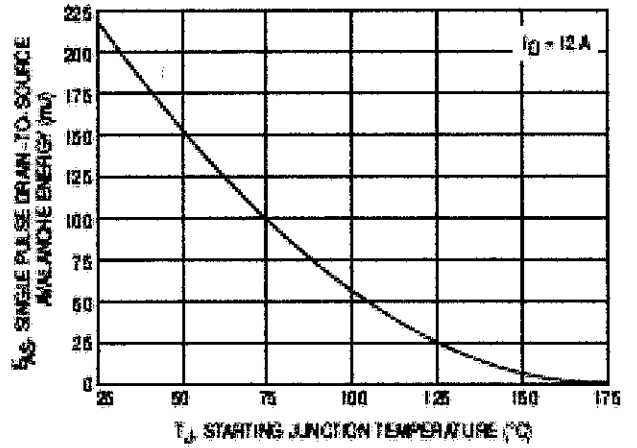


Figure 12. Maximum Avalanche Energy versus Starting Junction Temperature

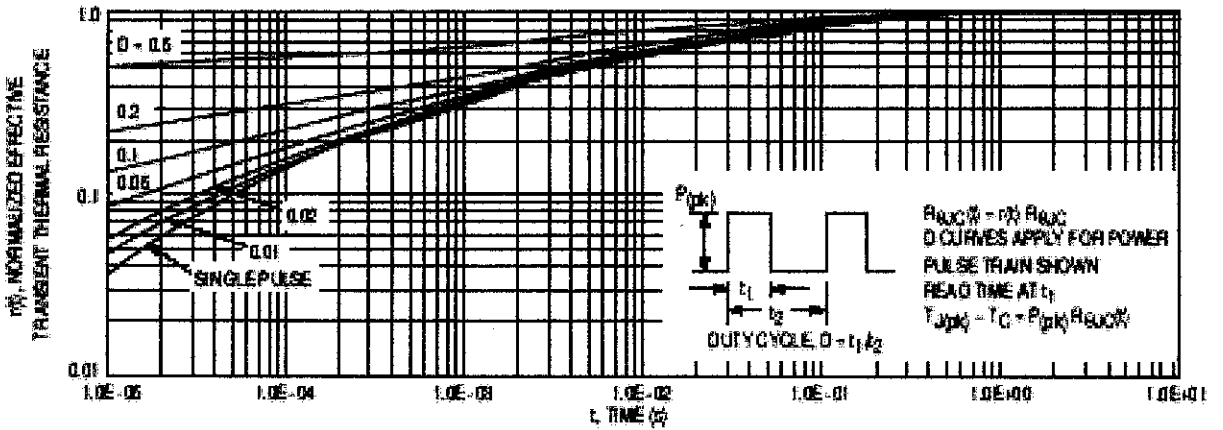


Figure 13. Thermal Response

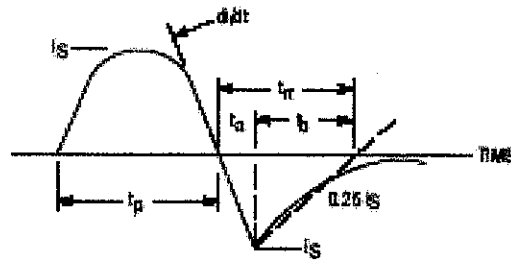
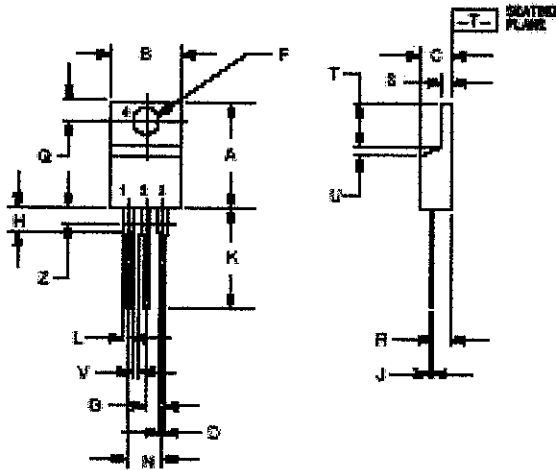


Figure 14. Diode Reverse Recovery Waveform

MTP2955V

PACKAGE DIMENSIONS

TO-220 THREE-LEAD
TO-220AB
CASE 221A-09
ISSUE AA



NOTES:

1. DIMENSIONING AND TOLERANCING PER ANSI Y14.5M, INC.
2. CONTROLLING DIMENSION IS INCH.
3. DIMENSION LOCOTRE IS A ZONE WHERE ALL BODY AND LEAD IRREGULARITIES ARE ALLOWED.

DIM	INCHES		MILLIMETERS	
	MIN	MAX	MIN	MAX
A	0.075	0.090	1.915	2.286
B	0.090	0.095	2.286	2.413
C	0.090	0.095	2.286	2.413
D	0.095	0.095	2.413	2.413
E	0.095	0.095	2.413	2.413
F	0.095	0.095	2.413	2.413
G	0.095	0.095	2.413	2.413
H	0.110	0.095	2.794	2.413
J	0.095	0.095	2.413	2.413
K	0.095	0.095	2.413	2.413
L	0.095	0.095	2.413	2.413
N	0.090	0.095	2.286	2.413
Q	0.090	0.095	2.286	2.413
R	0.090	0.110	2.286	2.794
S	0.095	0.095	2.413	2.413
T	0.095	0.095	2.413	2.413
U	0.090	0.090	2.286	2.286
V	0.095	--	2.413	--
Z	--	0.095	--	2.413

STYLE :

- 1. GATE
- 2. DOWN
- 3. SOURCE
- 4. DOWN

APPENDIX D

MTP3055V N-CHANNEL MOSFET DATASHEET

MTP3055V

Preferred Device

Power MOSFET 12 Amps, 60 Volts N-Channel TO-220

This Power MOSFET is designed to withstand high energy in the avalanche and commutation modes. Designed for low voltage, high speed switching applications in power supplies, converters and power motor controls, these devices are particularly well suited for bridge circuits where diode speed and commutating safe operating areas are critical and offer additional safety margin against unexpected voltage transients.

- On-resistance Area Product about One-half that of Standard MOSFETs with New Low Voltage, Low $R_{DS(on)}$ Technology
- Faster Switching than E-FET Predecessors
- Avalanche Energy Specified
- I_{DSS} and $V_{DS(on)}$ Specified at Elevated Temperature
- Static Parameters are the Same for both TMOS V and TMOS E-FET

MAXIMUM RATINGS ($T_C = 25^\circ\text{C}$ unless otherwise noted)

Rating	Symbol	Value	Unit
Drain-Source Voltage	V_{DS}	60	Vdc
Drain-Gate Voltage ($R_{GS} = 1.0\text{ M}\Omega$)	V_{DGR}	60	Vdc
Gate-Source Voltage	V_{GS}	± 20	Vdc
- Continuous	V_{GS}	± 25	Vpk
- Non-Repetitive ($t_p \leq 10\text{ ms}$)	V_{GSM}		
Drain Current - Continuous @ 25°C	I_D	12	Adc
- Continuous @ 100°C	I_D	7.3	
- Single Pulse ($t_p \leq 10\text{ }\mu\text{s}$)	I_{DM}	37	Apk
Total Power Dissipation @ 25°C	P_D	48	Watts
Derate above 25°C		0.32	$\text{W}/^\circ\text{C}$
Operating and Storage Temperature Range	T_J, T_{stg}	-55 to 175	$^\circ\text{C}$
Single Pulse Drain-to-Source Avalanche Energy - Starting $T_J = 25^\circ\text{C}$ ($V_{DD} = 25\text{ Vdc}$, $V_{GS} = 10\text{ Vdc}$, $I_L = 12\text{ Apk}$, $L = 1.0\text{ mH}$, $R_G = 25\text{ }\Omega$)	EAS	72	mJ
Thermal Resistance - Junction to Case	$R_{\theta JC}$	3.13	$^\circ\text{C}/\text{W}$
- Junction to Ambient	$R_{\theta JA}$	62.5	
Maximum Lead Temperature for Soldering Purposes, 1/8" from case for 10 seconds	T_L	260	$^\circ\text{C}$



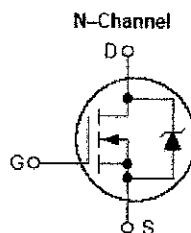
ON Semiconductor™

<http://onsemi.com>

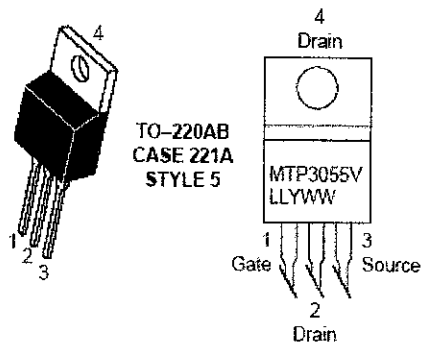
12 AMPERES

50 VOLTS

$R_{DS(on)} = 150\text{ m}\Omega$



MARKING DIAGRAM & PIN ASSIGNMENT



MTP3055V = Device Code
LL = Location Code
Y = Year
WW = Work Week

ORDERING INFORMATION

Device	Package	Shipping
MTP3055V	TO-220AB	50 Units/Rail

Preferred devices are recommended choices for future use and best overall value.

MTP3055V

ELECTRICAL CHARACTERISTICS (T_J = 25°C unless otherwise noted)

Characteristic	Symbol	Min	Typ	Max	Unit	
OFF CHARACTERISTICS						
Drain-Source Breakdown Voltage (V _{GS} = 0 Vdc, I _D = 250 μAdc) Temperature Coefficient (Positive)	V _{(BR)DSS}	60 -	- 65	-	Vdc mV/°C	
Zero Gate Voltage Drain Current (V _{DS} = 60 Vdc, V _{GS} = 0 Vdc) (V _{DS} = 60 Vdc, V _{GS} = 0 Vdc, T _J = 150°C)	I _{DSS}	-	-	10 100	μAdc	
Gate-Body Leakage Current (V _{GS} = ± 20 Vdc, V _{DS} = 0)	I _{GSS}	-	-	100	nAdc	
ON CHARACTERISTICS (Note 1.)						
Gate Threshold Voltage (V _{DS} = V _{GS} , I _D = 250 μAdc) Temperature Coefficient (Negative)	V _{GS(th)}	2.0 -	2.7 5.4	4.0 -	Vdc mV/°C	
Static Drain-Source On-Resistance (V _{GS} = 10 Vdc, I _D = 6.0 Adc)	R _{DS(on)}	-	0.10	0.15	Ohm	
Drain-Source On-Voltage (V _{GS} = 10 Vdc) (I _D = 12 Adc) (I _D = 6.0 Adc, T _J = 150°C)	V _{DS(on)}	-	1.3 -	2.2 1.9	Vdc	
Forward Transconductance (V _{DS} = 7.0 Vdc, I _D = 6.0 Adc)	g _{FS}	4.0	5.0	-	mhos	
DYNAMIC CHARACTERISTICS						
Input Capacitance	(V _{DS} = 25 Vdc, V _{GS} = 0 Vdc, f = 1.0 MHz)	C _{iss}	-	410	500	pF
Output Capacitance		C _{oss}	-	130	180	
Reverse Transfer Capacitance		C _{rss}	-	25	50	
SWITCHING CHARACTERISTICS (Note 2.)						
Turn-On Delay Time	(V _{DD} = 30 Vdc, I _D = 12 Adc, V _{GS} = 10 Vdc, R _G = 9.1 Ω)	t _{d(on)}	-	7.0	10	ns
Rise Time		t _r	-	34	60	
Turn-Off Delay Time		t _{d(off)}	-	17	30	
Fall Time		t _f	-	18	50	
Gate Charge (See Figure 8)	(V _{DS} = 48 Vdc, I _D = 12 Adc, V _{GS} = 10 Vdc)	Q _T	-	12.2	17	nC
		Q ₁	-	3.2	-	
		Q ₂	-	5.2	-	
		Q ₃	-	5.5	-	
SOURCE-DRAIN DIODE CHARACTERISTICS						
Forward On-Voltage (Note 1.)	(I _S = 12 Adc, V _{GS} = 0 Vdc) (I _S = 12 Adc, V _{GS} = 0 Vdc, T _J = 150°C)	V _{SD}	-	1.0 0.91	1.6 -	Vdc
Reverse Recovery Time (See Figure 15)	(I _S = 12 Adc, V _{GS} = 0 Vdc, di _S /dt = 100 A/μs)	t _{rr}	-	56	-	ns
		t _a	-	40	-	
		t _b	-	16	-	
Reverse Recovery Stored Charge		Q _R	-	0.128	-	μC
INTERNAL PACKAGE INDUCTANCE						
Internal Drain Inductance (Measured from contact screw on tab to center of die) (Measured from the drain lead 0.25" from package to center of die)	L _D	-	3.5 4.5	-	nH	
Internal Source Inductance (Measured from the source lead 0.25" from package to source bond pad)	L _S	-	7.5	-	nH	

1. Pulse Test: Pulse Width ≤ 300 μs, Duty Cycle ≤ 2%.
2. Switching characteristics are independent of operating junction temperature.

MTP3055V

TYPICAL ELECTRICAL CHARACTERISTICS

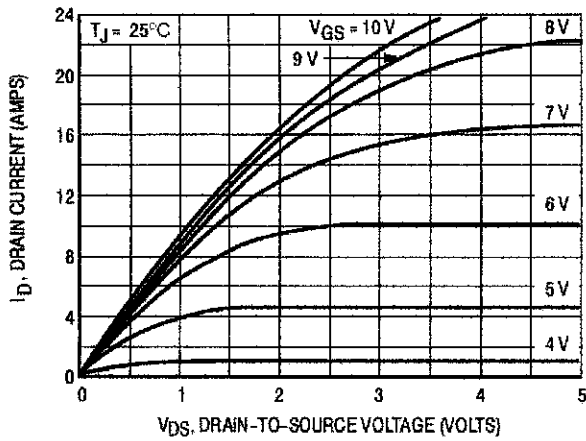


Figure 1. On-Region Characteristics

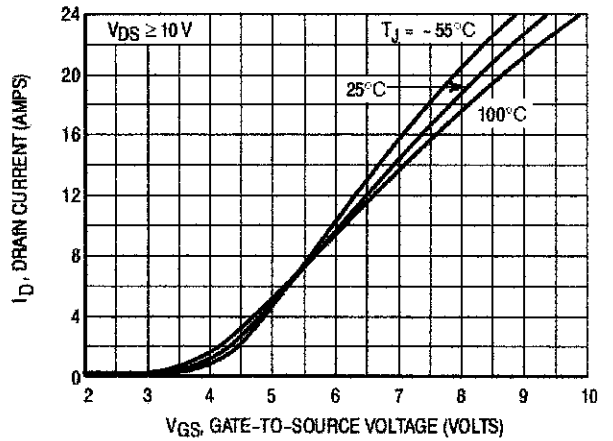


Figure 2. Transfer Characteristics

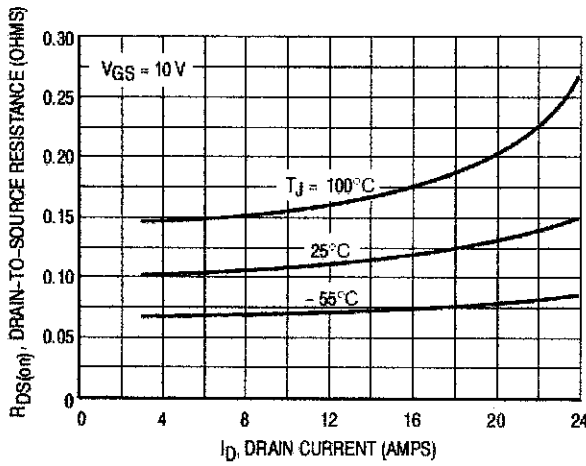


Figure 3. On-Resistance versus Drain Current and Temperature

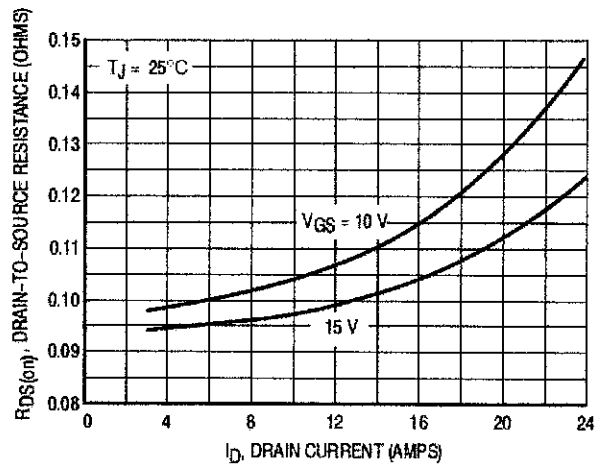


Figure 4. On-Resistance versus Drain Current and Gate Voltage

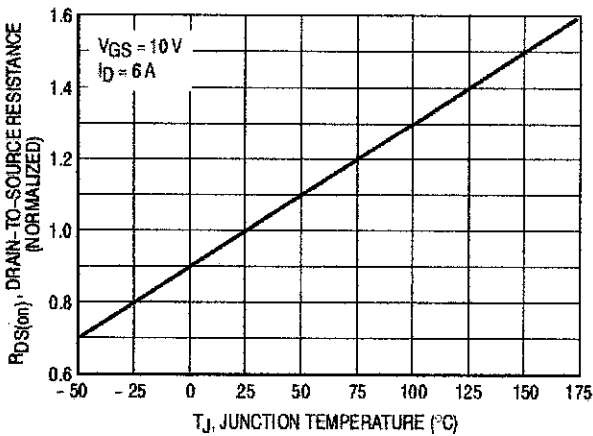


Figure 5. On-Resistance Variation with Temperature

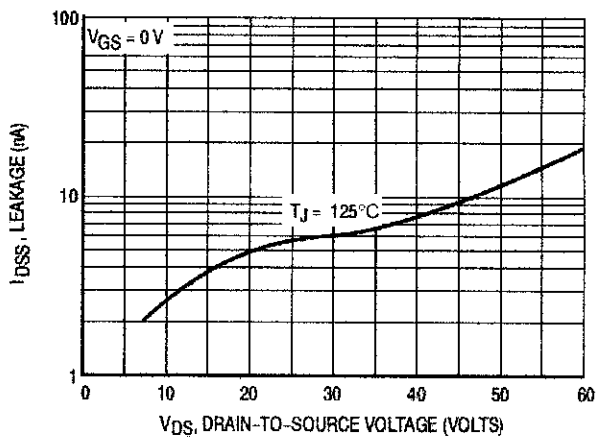


Figure 6. Drain-to-Source Leakage Current versus Voltage

MTP3055V

POWER MOSFET SWITCHING

Switching behavior is most easily modeled and predicted by recognizing that the power MOSFET is charge controlled. The lengths of various switching intervals (Δt) are determined by how fast the FET input capacitance can be charged by current from the generator.

The published capacitance data is difficult to use for calculating rise and fall because drain-gate capacitance varies greatly with applied voltage. Accordingly, gate charge data is used. In most cases, a satisfactory estimate of average input current ($I_{G(AV)}$) can be made from a rudimentary analysis of the drive circuit so that

$$t = Q/I_{G(AV)}$$

During the rise and fall time interval when switching a resistive load, V_{GS} remains virtually constant at a level known as the plateau voltage, V_{GSP} . Therefore, rise and fall times may be approximated by the following:

$$t_r = Q_2 \times R_G / (V_{GG} - V_{GSP})$$

$$t_f = Q_2 \times R_G / V_{GSP}$$

where

V_{GG} = the gate drive voltage, which varies from zero to V_{GG}

R_G = the gate drive resistance

and Q_2 and V_{GSP} are read from the gate charge curve.

During the turn-on and turn-off delay times, gate current is not constant. The simplest calculation uses appropriate values from the capacitance curves in a standard equation for voltage change in an RC network. The equations are:

$$t_{d(on)} = R_G C_{iss} \ln [V_{GG}/(V_{GG} - V_{GSP})]$$

$$t_{d(off)} = R_G C_{iss} \ln (V_{GG}/V_{GSP})$$

The capacitance (C_{iss}) is read from the capacitance curve at a voltage corresponding to the off-state condition when calculating $t_{d(on)}$ and is read at a voltage corresponding to the on-state when calculating $t_{d(off)}$.

At high switching speeds, parasitic circuit elements complicate the analysis. The inductance of the MOSFET source lead, inside the package and in the circuit wiring which is common to both the drain and gate current paths, produces a voltage at the source which reduces the gate drive current. The voltage is determined by $L di/dt$, but since di/dt is a function of drain current, the mathematical solution is complex. The MOSFET output capacitance also complicates the mathematics. And finally, MOSFETs have finite internal gate resistance which effectively adds to the resistance of the driving source, but the internal resistance is difficult to measure and, consequently, is not specified.

The resistive switching time variation versus gate resistance (Figure 9) shows how typical switching performance is affected by the parasitic circuit elements. If the parasitics were not present, the slope of the curves would maintain a value of unity regardless of the switching speed. The circuit used to obtain the data is constructed to minimize common inductance in the drain and gate circuit loops and is believed readily achievable with board mounted components. Most power electronic loads are inductive; the data in the figure is taken with a resistive load, which approximates an optimally snubbed inductive load. Power MOSFETs may be safely operated into an inductive load; however, snubbing reduces switching losses.

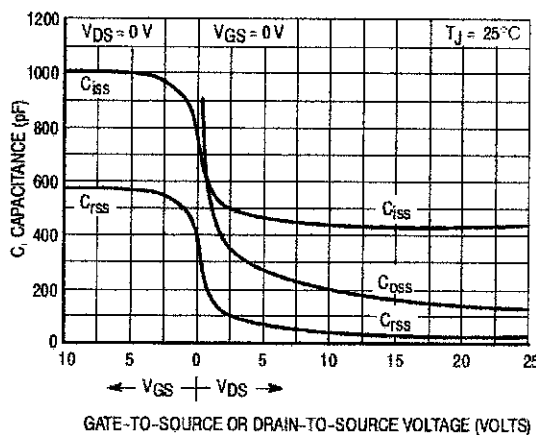


Figure 7. Capacitance Variation

MTP3055V

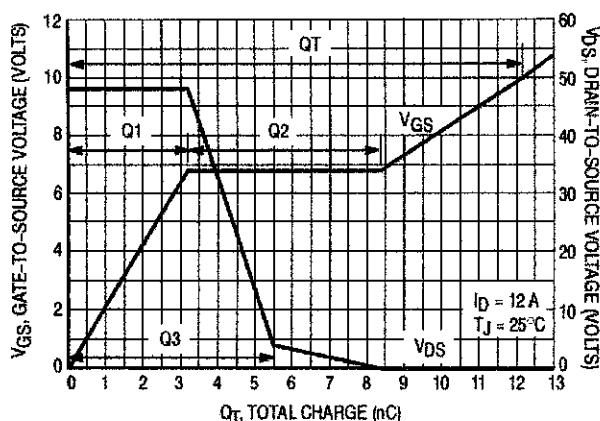


Figure 8. Gate-To-Source and Drain-To-Source Voltage versus Total Charge

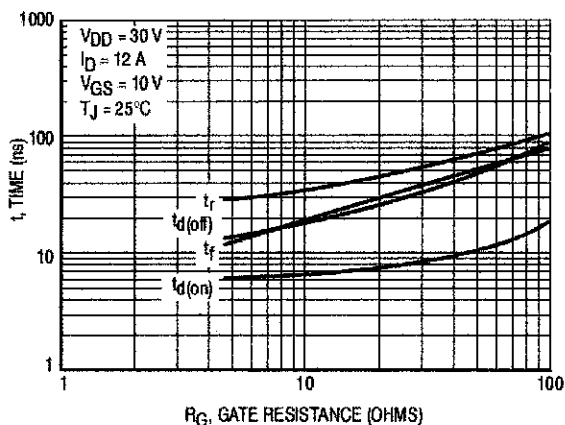


Figure 9. Resistive Switching Time Variation versus Gate Resistance

DRAIN-TO-SOURCE DIODE CHARACTERISTICS

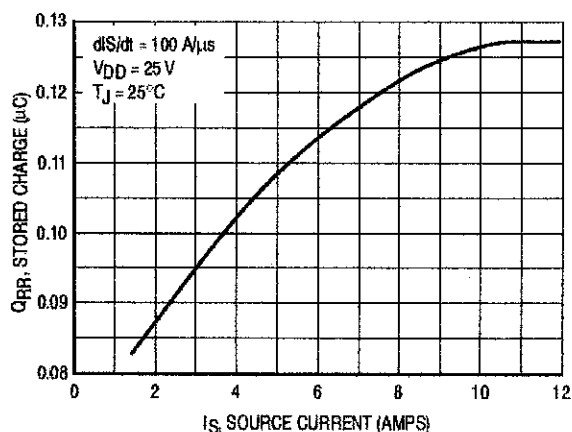


Figure 10. Stored Charge

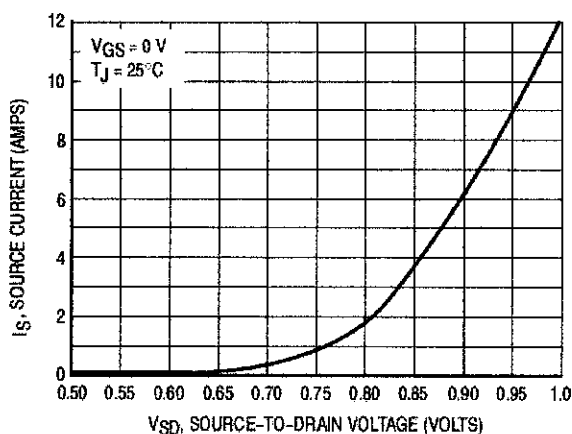


Figure 11. Diode Forward Voltage versus Current

SAFE OPERATING AREA

The Forward Biased Safe Operating Area curves define the maximum simultaneous drain-to-source voltage and drain current that a transistor can handle safely when it is forward biased. Curves are based upon maximum peak junction temperature and a case temperature (T_C) of 25°C. Peak repetitive pulsed power limits are determined by using the thermal response data in conjunction with the procedures discussed in AN569, "Transient Thermal Resistance—General Data and Its Use."

Switching between the off-state and the on-state may traverse any load line provided neither rated peak current (I_{DM}) nor rated voltage (V_{DSS}) is exceeded and the transition time (t_r, t_f) do not exceed 10 μ s. In addition the total power averaged over a complete switching cycle must not exceed $(T_{J(MAX)} - T_C)/(R_{\theta JC})$.

A Power MOSFET designated E-FET can be safely used in switching circuits with unclamped inductive loads. For

reliable operation, the stored energy from circuit inductance dissipated in the transistor while in avalanche must be less than the rated limit and adjusted for operating conditions differing from those specified. Although industry practice is to rate in terms of energy, avalanche energy capability is not a constant. The energy rating decreases non-linearly with an increase of peak current in avalanche and peak junction temperature.

Although many E-FETs can withstand the stress of drain-to-source avalanche at currents up to rated pulsed current (I_{DM}), the energy rating is specified at rated continuous current (I_D), in accordance with industry custom. The energy rating must be derated for temperature as shown in the accompanying graph (Figure 13). Maximum energy at currents below rated continuous I_D can safely be assumed to equal the values indicated.

MTP3055V

SAFE OPERATING AREA

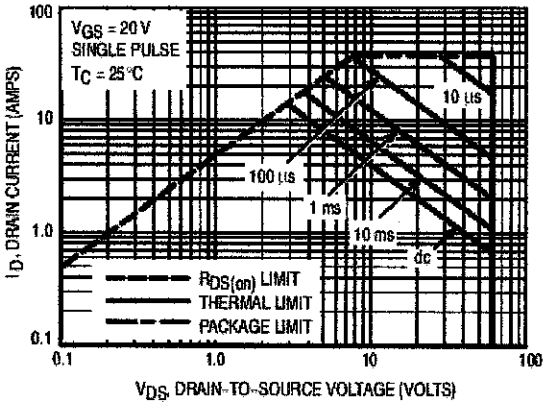


Figure 12. Maximum Rated Forward Biased Safe Operating Area

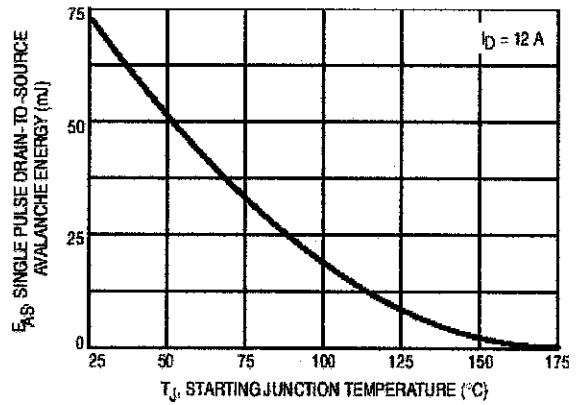


Figure 13. Maximum Avalanche Energy versus Starting Junction Temperature

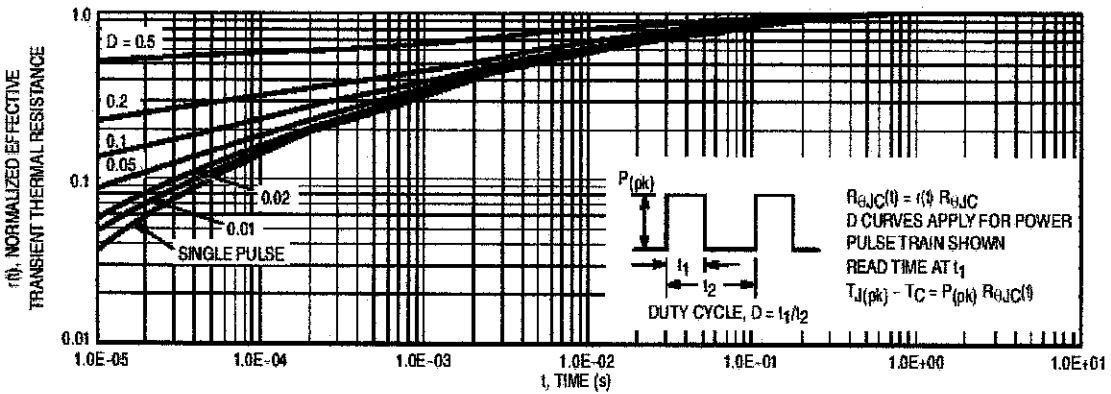


Figure 14. Thermal Response

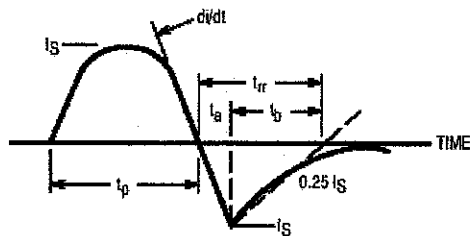
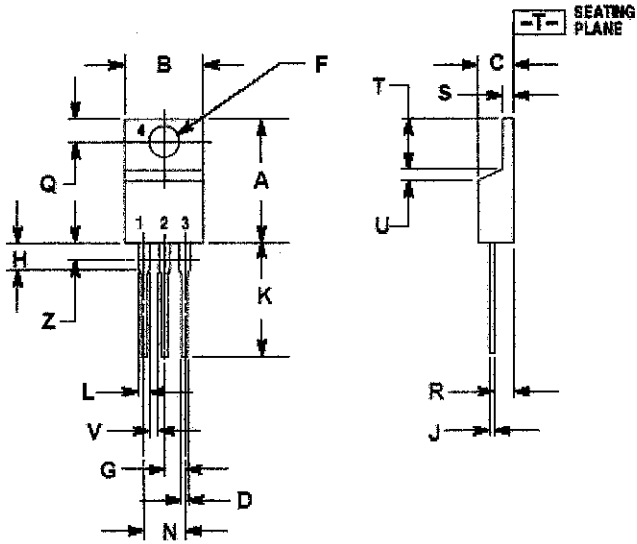


Figure 15. Diode Reverse Recovery Waveform

MTP3055V

PACKAGE DIMENSIONS

TO-220 THREE-LEAD
TO-220AB
CASE 221A-09
ISSUE AA



NOTES:

1. DIMENSIONING AND TOLERANCING PER ANSI Y14.5M, 1982.
2. CONTROLLING DIMENSION: INCH.
3. DIMENSION Z DEFINES A ZONE WHERE ALL BODY AND LEAD IRREGULARITIES ARE ALLOWED.

DIM	INCHES		MILLIMETERS	
	MIN	MAX	MIN	MAX
A	0.570	0.620	14.48	15.75
B	0.380	0.405	9.66	10.28
C	0.160	0.190	4.07	4.82
D	0.025	0.035	0.64	0.89
F	0.142	0.147	3.61	3.73
G	0.095	0.105	2.42	2.66
H	0.110	0.155	2.80	3.93
J	0.018	0.025	0.46	0.64
K	0.500	0.562	12.70	14.27
L	0.045	0.060	1.15	1.52
N	0.190	0.210	4.83	5.33
Q	0.100	0.120	2.54	3.04
R	0.080	0.110	2.04	2.79
S	0.045	0.055	1.15	1.39
T	0.235	0.255	5.97	6.47
U	0.000	0.040	0.00	1.27
V	0.045	---	1.15	---
Z	---	0.080	---	2.04

STYLE 5:

1. GATE
2. DRAIN
3. SOURCE
4. DRAIN